A matter of delivery: nanocarriers and the engineering of protective immunity in tuberculosis vaccination

Szachniewicz, M.M.

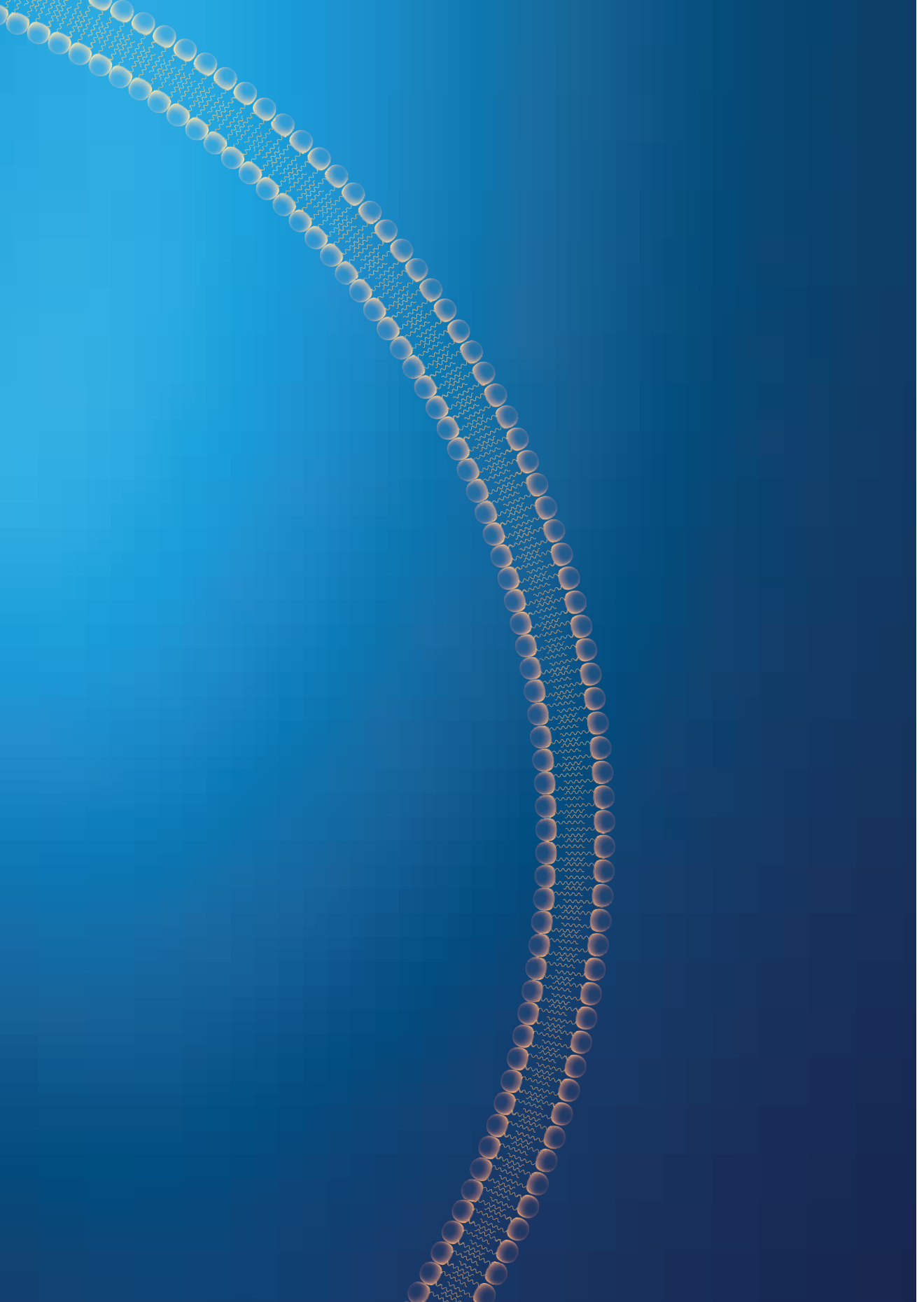

CHAPTER 4

Cationic pH-sensitive liposome-based subunit tuberculosis vaccine induces protection in mice challenged with Mycobacterium tuberculosis

M.M. Szachniewicz, S.J.F. van den Eeden, K.E. van Meijgaarden,
K.L.M.C. Franken, S. van Veen, A. Geluk, J.A. Bouwstra, T.H.M. Ottenhoff

Adapted from European Journal of Pharmaceutics and Biopharmaceutics, 2024, 203: 114437

ABSTRACT

Tuberculosis (TB) has been and still is a global emergency for centuries. Prevention of disease through vaccination would have a major impact on disease prevalence, but the only available current vaccine, BCG, has insufficient impact. In this article, a novel subunit vaccine against TB was developed, using the Ag85B-ESAT6-Rv2034 fusion antigen, two adjuvants – CpG and MPLA, and a cationic pH-sensitive liposome as a delivery system, representing a new TB vaccine delivery strategy not previously reported for TB.

In vitro in human dendritic cells (DCs), the adjuvanted formulation induced a significant increase in the production of (innate) cytokines and chemokines compared to the liposome without additional adjuvants. *In vivo*, the new vaccine administrated subcutaneously significantly reduced *Mycobacterium tuberculosis (Mtb)* bacterial load in the lungs and spleens of mice, significantly outperforming results from mice vaccinated with the antigen mixed with adjuvants without liposomes. In-depth analysis underpinned the vaccine's effectiveness in terms of its capacity to induce polyfunctional $CD4^+$ and $CD8^+$ T-cell responses, both considered essential for controlling Mtb infection. Also noteworthy was the differential abundance of various $CD69^+$ B-cell subpopulations, which included IL17-A-producing B cells. The vaccine stimulated robust antigen-specific antibody titers, further extending its potential as a novel protective agent against TB.

1. INTRODUCTION

TB remains one of the top infectious killers globally for decades. According to the WHO, TB is ranked as the 13th leading cause of all deaths worldwide, only during 2020-2021 second to COVID-19 as the deadliest infectious disease.[1] TB was responsible for 1.3 million deaths in 2022 alone.[2] Goals set by the End TB Strategy involve early TB diagnostics, including new point-of-care tests, safer and shorter medication regimens, safer and more effective therapy of latent TB, and, in particular, effective pre- and post-exposure vaccination.[3] To this day there is only one approved TB vaccine – *Mycobacterium bovis* Bacillus Calmette–Guérin (BCG). The major shortcoming of BCG is its highly variable efficacy, ranging from 0 to 80 %, and its limited induction of protection to infectious pulmonary TB in adults.[4] Therefore, there is a need for novel, more effective vaccines.

Vaccines are prepared using attenuated, inactivated, recombinant pathogens or derived substances from these pathogens, also known as subunit vaccines.[5] The first three categories of vaccines can induce robust immune responses; however, there are also associated health risks, including mutation, reversion, and contamination.[6,7] In contrast, subunit vaccines (proteins, lipids, RNA, DNA, etc.) are less immunogenic, but the safety concerns are significantly reduced thanks to their synthetic nature. Subunit vaccines are versatile, and most aspects can be easily modified and optimized for specific types of immune responses. Weak immunogenicity can be overcome by adjuvants that induce robust and specific types of immune responses and delivery systems that allow increased uptake of antigens and adjuvants by professional antigen-presenting cells (APCs) such as DCs and macrophages.[7]

Vaccine delivery systems are thus excellent tools to increase the immunogenicity of subunit vaccines, increase the uptake of antigens and adjuvants by APCs, and thus help decrease and "spare" vaccine doses and costs. Cationic liposomes are widely researched vaccine delivery systems. They are intrinsically immunogenic, rapidly taken up by APCs, and easy to customize regarding their physicochemical properties like size, charge, bilayer organization, and surface chemistry. They can be formulated with various molecular adjuvants and antigens including peptides, proteins, RNA, and DNA.[8–12]

Cationic pH-sensitive liposomes are a unique type of delivery system characterized by their responsiveness to changes in the pH of the environment. At the physiological pH, the liposomes are stable; however, when internalized by APCs and exposed to decreasing pH inside endosomes, their liposomal bilayer becomes unstable. The destabilized lipid phase fuses with the endosomal membrane, which makes it leaky and allows it to release the content of the endosome into the cytosol.[13–16] This has potential benefits for vaccination. It prevents the degradation of antigens carried by the liposome inside the endosome and consequently facilitates MHC class I antigen presentation leading to increased cytotoxic $CD8^+$ T-cell responses.[13,16–18] pH-sensitive liposomes have not been widely studied for vaccination against infectious diseases. In literature, pH-sensitive liposomes are studied primarily in gene delivery and gene-based cancer vaccines.[13,19–23] Here, we explored the application of pH-sensitive liposomes as a subunit (fusion-protein-based) vaccine delivery system against TB.

In this study, we used cationic pH-sensitive liposomes to deliver a triple fusion antigen protein Ag85B-ESAT6-Rv2034 (AER), and molecular adjuvants cytosine-phosphate-guanine motifs (CpG) (ODN1826) and a synthetic monophosphoryl lipid A (MPLA). Ag85B and ESAT6 are immunodominant antigens abundantly expressed at an early stage of Mtb infection. Both antigens are extensively studied in TB vaccine research.[5,24,25] Notably, both are currently used in vaccines in clinical trials: H1:IC31[25] and H56:IC31 (H56 also contains Rv2660c antigen).[26] Rv2034 has been identified as a potent *in vivo* expressed Mtb antigen.[27] It was shown effective in inducing protection against Mtb in HLA-DR3 transgenic mice.[25] AER fusion protein combined with cationic adjuvant formulation 09 (CAF09) effectively reduced bacterial burden in HLA-DR3 transgenic mice and guinea pigs CpG is a Toll-like receptor (TLR) 9 ligand that induces strong Th1 immune responses in mice, and it was previously shown as an effective adjuvant for the Rv2034-based subunit vaccine.[25] MPLA (PHAD) is a synthetic analog of naturally occurring MPLA, which is a potent TLR4 agonist that induces Th1 as well as Th17 responses.[28–30]

MPLA and CpG have been used together in a liposomal vaccine adjuvant called AS15, which consists of *Quillaja saponaria Molina*, fraction 21 (QS-21), MPLA, and CpG 7909. Intramuscular administration of AS15 in mice induced activation of DCs, as indicated by cell-surface activation markers CD40, CD80, and CD86 on DCs in draining lymph nodes.[31] Several phase II and III clinical trials demonstrated that cancer vaccines (melanoma and non-small-cell lung cancer) utilizing this adjuvant

system were safe and induced robust, specific T-cell and antibody responses.[31–35] Compared to a similar adjuvant AS02B that does not include CpG, AS15 was shown to induce superior immune responses.[34] Further development of these vaccines has been discontinued because of the lack of efficacy in two phase III trials. However, the body of evidence indicates that a combination of MPLA and CpG in a liposomal formulation is an effective and safe system for inducing robust immune responses and it is worth further investigation.

In this work, we developed a new tuberculosis subunit vaccine using DOPC:DOPE:DOBAQ:EPC 3:5:2:4 pH-sensitive liposomes as a delivery system for AER, CpG, and MPLA. We evaluated its efficacy *in vitro* using primary human monocyte-derived dendritic cells to evaluate its immunogenicity and *in vivo* using C57Bl/6 mice mucosal Mtb infection model to investigate induction of protection in terms of reduction of colony forming units (CFUs) in lungs and spleens of mice challenged with H37Rv Mtb strain, and immune responses in vaccinated non-Mtb-challenged mice, using a 27 marker spectral flow cytometry panel for analysis of $CD4^+$, $CD8^+$ T-cells, and B-cell responses, as well as antigen-specific antibody titers in sera. To identify differentially abundant and biologically relevant populations of cells followed by vaccinations, we performed dimension reduction analyses.

2. MATERIALS AND METHODS

2.1 Materials

1,2-dioleoyl-sn-glycero-3-phosphocholine (DOPC), 1,2-dioleoyl-sn-glycero-3-ethyl-phosphocholine chloride salt (EPC), 1,2-dioleoyl-sn-glycero-3-phosphoethanolamine (DOPE), N-(4-carboxybenzyl)-N,N-dimethyl-2,3-bis(oleoyloxy)propan-1-aminium (DOBAQ) and monophosphoryl lipid A (PHAD), synthetic (MPLA) were acquired from Avanti Polar Lipids, Inc. (USA). The chemical structures of the lipids are shown in Figure S1. Class B CpG oligonucleotide ODN1826 was obtained from InvivoGen (the Netherlands). Recombinant fusion protein AER was produced as described previously by Franken et al.[36] In brief, genes obtained from Mtb (lab strain H37Rv) were amplified through polymerase chain reaction (PCR) using genomic DNA. These amplified genes were cloned using Gateway technology (Invitrogen, USA) into bacteria containing an N-terminal hexahistidine (His) tag. The successful insertion of the cloned products was confirmed through sequencing. Next, the antigen AER was

expressed in *Escherichia coli* strain BL21 (DE3) and subsequently purified. Produced AER was subsequently purified. The protein quality, size, purity, and determination of endotoxin concentration were performed as described by Franken et al.[36]

2.2 Liposome preparation

Liposomes were prepared using the thin-film hydration method as described previously.[37] Lipids were dissolved in chloroform, with appropriate lipids diluted from 25 mg/ml stock solutions. A total of 10 mg (10 mg/ml) lipids in chloroform were used per batch. The lipid solution was added into a round-bottom flask, and the chloroform was removed by evaporation for 1 hour using a Buchi rotavapor R210 (Switzerland). The lipid film was flushed with nitrogen for 5 minutes to remove any remaining traces of chloroform and rehydrated with 1 ml of 200 µg/ml AER in 10 mM phosphate buffer (PB) at pH 7.4 to prepare AER-containing liposomes. Following rehydration, the liposomes were downsized using a Branson sonifier 250 (US) with an eight-cycle sonication program. Each cycle comprised 30 seconds of sonication at 10 % amplitude, followed by a 60-second break. The liposomes were subsequently centrifuged at 1500 RPM for 5 minutes (Allegra X-12R, US) to remove any metal particles released by the sonicator. The resulting liposomal suspensions were transferred to new tubes, discarding the pellet, 1 mg/ml CpG in water was added dropwise, and further diluted with PB. The final product contained 40 µg/ml AER, 12 µg/ml CpG, 2 mg/ml lipids, 5 µg/ml MPLA, and 10 mM PB. The liposomes were stored at 4 °C overnight and injected into mice the next day. For each immunization (three per experiment), a new batch of liposomes were produced, and their quality was assessed based on size, size distribution, and zeta-potential prior to injection.

2.3 Liposome characterization (size and zeta-potential)

The intensity-weighted average hydrodynamic diameter (Z-average size) and polydispersity index (PDI) of the liposomal formulations were determined using dynamic light scattering (DLS), while the zeta potential was measured using laser Doppler electrophoresis. The liposomes were diluted to 0.25 mg/mL lipid concentration in 10 mM phosphate buffer (PB) at pH 7.4 to perform the measurements. The diluted liposomes were transferred to 1.5 ml VWR Two-Sided Disposable PS Cuvettes (VWR, the Netherlands). Each batch was measured in triplicates, with a minimum of ten runs per measurement at a temperature of 20 °C. A Nano ZS Zetasizer equipped

with a 633 nm laser and 173° optics (Malvern Instruments, Worcestershire, UK) was employed for the DLS and zeta potential measurements. The acquired data were analyzed using Zetasizer Software v7.13 (Malvern Instruments).

2.4 Mice

C57Bl/6 mice were obtained from The Jackson Laboratory (ME, USA) (stock number SC1300004) and were housed in the animal facilities of the Leiden University Medical Center (LUMC), the Netherlands. Female mice 6-8 weeks old at the start of each experiment were used. All Mtb infections were performed in a biosafety level 3 (BSL-3) facility at the LUMC.

All mouse experiments were individually designed, reviewed, ethically approved, and registered the LUMC's institutional Animal Welfare Body, and executed under the project license number AVD116002017856, which was granted by the Netherlands' authoritative body on animal experimentation, the CCD. These experiments adhered strictly to the Dutch Act on Animal Experimentation regulations and the European Union Directive 2010/63/EU, at the LUMC facility. The mice were kept in separately ventilated cages, maintaining a maximum occupancy of six mice per cage, and the studies commenced only after an acclimatization period of one-week post-transport.

2.5 Immunizations

Mice (6 mice per group per experiment) were vaccinated with either BCG or AER solution mixed with CpG (ODN1826) and MPLA (PHAD) or liposomes. For liposome immunization, mice were injected 3 times with liposomal suspension (each dose containing 8 µg AER, 400 µg total lipids, 2.5 µg CpG ODN1826, and 1 µg MPLA (PHAD) in 200 µl of PB) subcutaneously (s.c.) in the right flank at 2 weeks intervals. Four weeks after the last immunizations, mice were sacrificed or infected with live Mtb. For immunization with AER mixed with adjuvants, mice were injected 3 times s.c. with AER mixed with CpG and MPLA in phosphate-buffered saline (each dose containing 25 µg AER, 50 µg CpG, and 1 µg MPLA in 200 µl PBS) in the right flank at 2 weeks interval, as described by Commandeur et al.[25] The liposomal immunization used a 3 times lower dose of AER and 20 times lower dose of CpG to evaluate whether reducing the dose using vaccine delivery technology is possible and effective compared to work by Commandeur et al.[25] For BCG immunization, mice were once injected s.c. 12 weeks before sacrificing or infection with live Mtb, in the

right flank with 10^6 CFU live BCG (Danish strain 1331) from glycerol stocks, stored at -80 °C. The number of bacteria was determined by plating the suspension used for infection on 7H10 agar plates (Difco, BD, Franklin Lakes, NJ USA) supplemented with BBL Middlebrook OADC enrichment (BD, Franklin Lakes, NJ USA). Colonies were counted after 3 weeks of incubation at 37 °C.

2.6 Intranasal infection with live Mtb

Naïve and immunized mice were infected with live Mtb strain H37Rv 4 weeks after third liposome immunization or 12 weeks after BCG immunization. Mice were anesthetized with isoflurane (2-chloro-2-(difluoromethoxy)-1,1,1-trifluoroethane; Pharmachemie BV, The Netherlands) and intranasally (i.n.) infected with 10^5 CFU Mtb from glycerol stocks, stored at -80 °C.[38] Plating the suspension used for infection on 7H10 agar plates determined the number of bacteria. Colonies were counted after 3 weeks of incubation at 37 °C.

Mice were euthanized with CO_2, 6 weeks post Mtb infection, and spleens and lungs were aseptically removed. The organs were homogenized using 70 µM cell strainers (Corning, USA) in sterile PBS, and the bacterial load was determined by plating in serial dilutions on 7H11 agar plates (BD Bioscience, USA), supplemented with OADC, and PANTA (BD, Franklin Lakes, NJ USA).

2.7 *In vitro* cultures

Splenocytes of immunized uninfected mice were resuspended at 3×10^6 cells/ml in Iscove's Modified Dulbecco's Medium (IMDM) (Gibco, Thermo Fisher Scientific, Belgium), supplemented with 2 mM GlutaMAX Supplement (Gibco, Thermo Fisher Scientific, Belgium), 100 U/100 µg/ml penicillin-streptomycin (Gibco, Paisley, UK), and 8 % heat-inactivated fetal bovine serum (FBS; Greiner, Frickenhausen, Deutschland) and *in vitro* stimulated with 5 µg/mL of fusion protein AER, at 37 °C 5 % CO_2. After 6 days, the splenocytes were restimulated with 5 µg/ml of the same protein as the stimulation for 5 hours, and 2.5 µg/mL Brefeldin A (Sigma, Merck, Darmstadt, Germany) was added for overnight incubation. Next, splenocytes were harvested and stained for intracellular cytokines and surface markers.

For cytokine production by restimulated splenocytes, 3×10^6 cells/ml were resuspended in IMDM, supplemented with 2 mM GlutaMAX Supplement, 100

U/100 µg/ml penicillin-streptomycin, and 8 % heat-inactivated FBS and incubated with the antigen in round bottom 96 wells plates. Supernatants were collected after 6 days.

2.8 Antibody enzyme-linked immunosorbent assay (ELISA)

Blood was collected from immunized uninfected mice via heart puncture upon sacrifice and stored on ice. Sera were obtained by blood centrifugation at 15,000 rpm for 10 minutes. Antibodies against proteins in sera were determined by ELISA: plates were coated overnight at 4 °C with protein (5 µg/ml) or PBS/0.4 % bovine serum albumin (BSA) (Sigma, Merck, Darmstadt, Germany), washed and blocked for 2 h using PBS/1 % BSA/1 % Tween-20. Serum dilutions (100 µl/well) were incubated at 37 °C for 2 h. Plates were washed (PBS, 0.05 % Tween-20) and incubated with 100 µl/well horse radish peroxide (HRP)-labeled, rabbit-anti-mouse total IgG, IgG1, IgG2a, IgG2b, IgG2c, IgG3 and IgM (Dako, Denmark). After 2 h at 37 °C, plates were washed and 100 µl/well tetramethylbenzidine substrate (TMB; Sigma) was added for 15 min at room temperature after which H_2SO_4 (1 M; 100 µl/well) was added and OD450 measured using Spectramax i3x spectrometer (Molecular Devices, CA, USA).

2.9 Antibody staining and flow cytometry

For flow cytometry analysis, the splenocytes were transferred into round-bottom 96-well plates (CELLSTAR, Greiner Bio-One GmbH, Germany) and washed with FACS buffer (PBS containing 0.1 % BSA; Sigma, Merck, Darmstadt, Germany). Next, the Zombie UV Fixable Viability Kit was reconstituted according to the manufacturer's instruction (BioLegend, the Netherlands), and the working solution was diluted 1:250 in PBS. 100 µl of the diluted dye was added to each well, and cells were incubated at room temperature in the dark for 30 minutes. Cells then were washed twice with FACS buffer. After that, cells were blocked with 20 µl of 5 % normal mouse serum (Thermo Fisher Scientific Inc., Bleiswijk, the Netherlands) in FACS buffer for 15 minutes at room temperature. Antibody staining was then performed. The list of antibodies used are listed in Table 1. Briefly, cells were washed once, and stained with CCR7 for 30 minutes at 37 °C. Next, cells were washed twice, and stained with 50 µl/well antibody mix containing remaining cell surface markers in FACS buffer containing 10 µl/well of BD Horizon Brilliant Stain Buffer Plus (BD Biosciences, Belgium). Cells were incubated at 4 °C for 30 minutes. Subsequently, cells were washed twice, and cells were fixated and permeabilized using eBioscience Foxp3/Transcription Factor

Staining Buffer Set (Invitrogen, Thermo Fisher Scientific, Belgium) at 4 °C for 60 minutes according to the manufacturer's instructions. After washing, intracellular staining was performed using an antibody mix diluted in a permeabilization buffer. Cells were incubated with 50 µl/well antibody mix at room temperature for 45 minutes. Afterward, cells were washed twice resuspended in 100 µl/well FACS buffer. Cells were stored at 4 °C until measured with a 5-laser Cytek Aurora spectral flow cytometer (Cytek Biosciences, Fremont, CA, USA) at the Flow cytometry Core Facility of Leiden University Medical Center (LUMC) in Leiden, the Netherlands.

Table 1. List of antibodies used in this study for spectral flow cytometry analysis of $CD4^+$, $CD8^+$, and $CD3^-$ $CD19^+$ B-cells.

Marker	Fluorochrome	Clone	Manufacturer
CCR7 (CD197)	PE/Cyanine5	4B12	BioLegend
CD273	BUV 395	TY25	BD Biosciences
CD8b.2	BUV 496	53-5.8	BD Biosciences
CD80	BUV 661	16-10A1	BD Biosciences
CD69	BUV 737	H1.2F3	BD Biosciences
CD25	BV 480	PC61	BD Biosciences
CD154	Super Bright 436	MR1	Thermo Fisher
IgD	Pacific Blue	11-26c.2a	BioLegend
I-A/I-E (MHC class II)	BV 510	M5/114.15.2	BioLegend
CD44	BV 570	IM7	BioLegend
PD-1 (CD279)	BV 605	29F.1A12	BioLegend
CXCR3 (CD183)	BV 650	CXCR3-173	BioLegend
KLRG1 (MAFA)	BV 711	2F1/KLRG1	BioLegend
CCR6 (CD196)	BV 785	29-2L17	BioLegend
CD4	Spark Blue 550	GK1.5	BioLegend
CCR5 (CD195)	PerCP/Cyanine5.5	HM-CCR5	BioLegend
CD19	PE Fire 640	6D5	BioLegend
CD138	APC	281-2	BioLegend
B220 (CD45R)	Spark NIR 685	RA3-6B2	BioLegend

CD62L (L-selectin)	APC/Fire 750	MEL-14	BioLegend
CD3	APC/Fire 810	17A2	BioLegend
IL-2	APC-R700	JES6-5H4	BD Biosciences
IL-17A	PE	eBio17B7	Thermo Fisher
IgM	FITC	RMM-1	BioLegend
IL-10	PE/Dazzle 594	JES5-16E3	BioLegend
TNFα	PE/Cyanine7	MP6-XT22	BioLegend
IFNγ	Alexa Fluor 647	XMG1.2	BioLegend

2.10 Analysis of flow cytometry data

Data were analyzed using FlowJo v10.8.0 and OMIQ analysis software (www.omiq.ai). The analysis strategy is depicted in Figure S2. Briefly, using FlowJo the data were first manually gated to remove debris, doublets, acquisition-disturbed events, and dead cells. Subsequently, cells were gated on CD3 vs CD19, and $CD3^+$ $CD19^-$ (T-cells) and $CD3^-$ $CD19^+$ (B-cells) were separately exported (minimum 20,000 events each population) and uploaded to the OMIQ platform (Figure S2). Imported data were further cleaned with the FlowAI tool in OMIQ. UMAP was performed on digitally concatenated cells. Subsequently, single marker gates were created for all markers except live/dead stain, CD3 (Figure S3), and CD19 (Figure S4). Using Boolean gating, combinations of gates were created. Afterward, counts for all Boolean gates were exported, and statistical analysis was performed.

2.11 Statistical analysis

Mann-Whitney statistical test with Benjamini Hochberg false discovery rate (FDR) correction was carried out using R[39] and RStudio,[40] to identify differentially abundant populations of cells. In GraphPad Prism, version 8.01 (GraphPad software, Prism, USA) statistical analyses were performed to compare vaccination groups. The results were analyzed with the Kruskal-Wallis test followed by an uncorrected Dunn's post-hoc test when comparing non-parametric data sets of three or more groups to the control group, where $P < 0.05$ was considered as statistically significant (*$P < 0.05$, **$P < 0.01$, ***$P < 0.001$, ****$P < 0.0001$). Graph values represent the median and error bars the interquartile range (IQR) unless indicated otherwise.

3. RESULTS

In this study, DOPC:DOPE:DOBAQ:EPC 3:5:2:4 cationic pH-sensitive liposomal formulation was used to deliver AER antigen, which was previously described as very promising *in vitro* (Szachniewicz, submitted [Chapter 3]). Based on our previous research, this liposome was an excellent candidate for further testing *in vivo*. To further increase the activation of APCs *in vivo*, two TLR agonists CpG and MPLA were incorporated.

3.1 Characterization of the vaccine formulation

The pH-sensitive liposomal formulation with CpG and MPLA was prepared, and its physicochemical properties were measured. The size of the prepared liposomes was 164.6 ± 33.1 nm, PDI 0.30 ± 0.10, and Zeta-potential 21.4 ± 2.5 mV. The values represent a mean and standard deviation of three independent batches.

3.2 Immunogenicity of the vaccine formulation in primary human MDDCs model

First, the effect of DOPC:DOPE:DOBAQ:EPC liposome formulated with AER, CpG, and MPLA on cytokine production in primary human MDDCs was investigated (Figure S5). The adjuvanted formulation induced a significant increase in the production of IL-1RA, IL-6, TNFα, CCL2, CCL3, CCL4, CCL5, CCL8, CCL11, CCL22, CXCL9, and CXCL10. These results supported the hypothesis that the formulation could effectively stimulate APCs and induce innate and also adaptive immune responses (see further below) to AER. Furthermore, the immunogenicity of liposomes containing different doses of AER (5 µg/ml, 1.5 µg/ml, and 0.5 µg/ml), CpG, and MPLA was evaluated using flow cytometry to investigate their effect on the expression of cell surface activation markers (CD40, CD80, CD83, and CD86) and cytotoxicity (Figure S6). All liposome formulations significantly upregulated the expression of these markers, and no cytotoxicity was observed. The effect of incorporating molecular adjuvants CpG and MPLA was further evaluated with this method (Figure S7). The combination of CpG and MPLA significantly increased CD80, CD83, and CD86 expression but not CD40. The adjuvant-free liposomal vaccine increased CD40 and CD83 but did not increase CD80 and CD86. In contrast, the liposome formulated with both CpG and MPLA increased all these cell surface markers, demonstrating the excellent immunogenicity of this formulation *in vitro*.

3.3 pH-sensitive liposome-based vaccine induced protection in mice

The efficacy of the vaccines to induce protection in mice was investigated. Immunization groups are summarized in Table 2. We assessed the bacterial burden in lungs and spleens of mice six weeks after the infection (Figure 1). CFUs from mice vaccinated with the pH-sensitive liposomal vaccine and BCG were significantly reduced compared to unimmunized mice both in lungs and spleens. Compared to the liposomal vaccine, mice immunized with AER mixed with adjuvants without liposomal constituents, showed bacterial reduction only in spleens but not in lungs. Importantly, the liposomal vaccine reduced CFUs significantly better in spleens compared to the non-liposomal formulation. The data show a notable range in the bacterial burden, indicating variable immune responses among the mice. Noteworthy is that in 6 mice of the BCG-vaccinated group and 2 mice of the pH-sensitive liposome group, the CFUs were at the detection limit of 100-200 CFUs, which is over 10^3 times less in lungs and over 10^4 times less in spleens compared to CFUs of unimmunized mice. These results indicate a high level of protection. Only 1 mouse of the AER-adjuvant mix group showed such a level of protection, but it was limited to lungs and not in spleens. Furthermore, the protection using the cationic pH-sensitive formulation was achieved using 3 times lower dose of the antigen and 20 times lower dose of CpG, demonstrating significant benefits using these liposomes.

Table 2. Summary of vaccination groups and doses of vaccine constituents administrated to a mouse per single immunization.

Group	Description	AER (µg)	Liposome (µg)	CpG (µg)	MPLA (µg)
Naïve	Unimmunized	NA	NA	NA	NA
BCG	Applied human vaccine	NA	NA	NA	NA
Ag	Antigen-adjuvant mix	25	NA	50	1
pH	pH-sensitive liposome	8	400	2.5	1

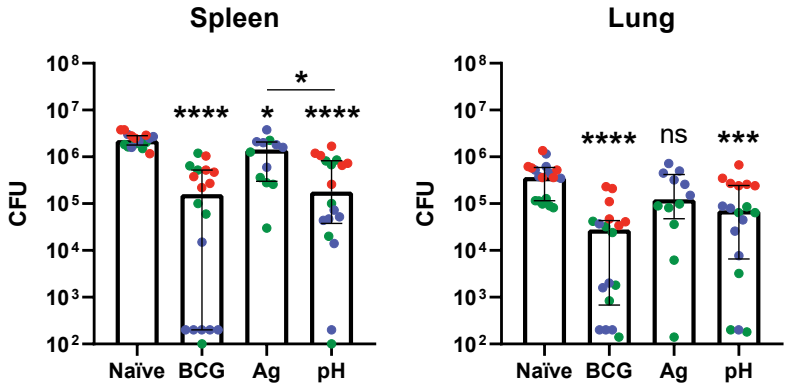

Figure 1. Bacterial burden in spleens (a) and lungs (b) of challenged mice represented with colony forming units (CFU) of Mtb. Each point represents CFU obtained from a single mouse. n = 18 except Ag group n = 12. Median ± IQR. Each dot represents a single mouse and results from the same experiment are shown in one color. Groups represent: naïve – unimmunized mice, BCG – BCG vaccination, Ag – AER/CpG/MPLA mixture vaccination, pH – vaccination with cationic pH-sensitive liposomal formulation of AER/CpG/MPLA. The statistical analysis shown compares to the naïve mice unless otherwise indicated.

3.4 The abundance of polyfunctional CD4⁺ T-cells increased after vaccination

To explore the immune responses induced by the vaccine, we evaluated the phenotypical abundance of various lymphocyte populations. First, we visually investigated differences in the abundance of $CD4^+$ and $CD8^+$ T-cell subsets between different immunization groups by UMAP (Figure 2). To quantitively analyze those differences, a differential subset abundance analysis was performed to identify populations of interest. The criteria for selecting cell subsets were: sufficiently large (> 100 events) and expressed biologically relevant marker profiles, enabling the identification of specific immune response populations. If several subpopulations had overlapping marker expression patterns, we selected one that is defined by more markers or had a lower p-value. We observed several $CD4^+$ T-cell subpopulations with polyfunctional phenotypes (Figure 3). The largest polyfunctional population defined as $CD4^+$ IL-2^+ $IFN\gamma^+$ $TNF\alpha^+$ IL-$17A^-$ IL-10^- $CD44^-$ $CD62L^+$ $CCR7^-$ T-cells. This population was more than twice as abundant in mice vaccinated with AER mixed with adjuvants and with the liposomal formulation, compared to naïve and BCG-vaccinated mice, and, importantly, also displayed a central memory phenotype. Secondly, a much less abundant population of IFNγ-producing $CD4^+$ IL-2^- $IFN\gamma^+$

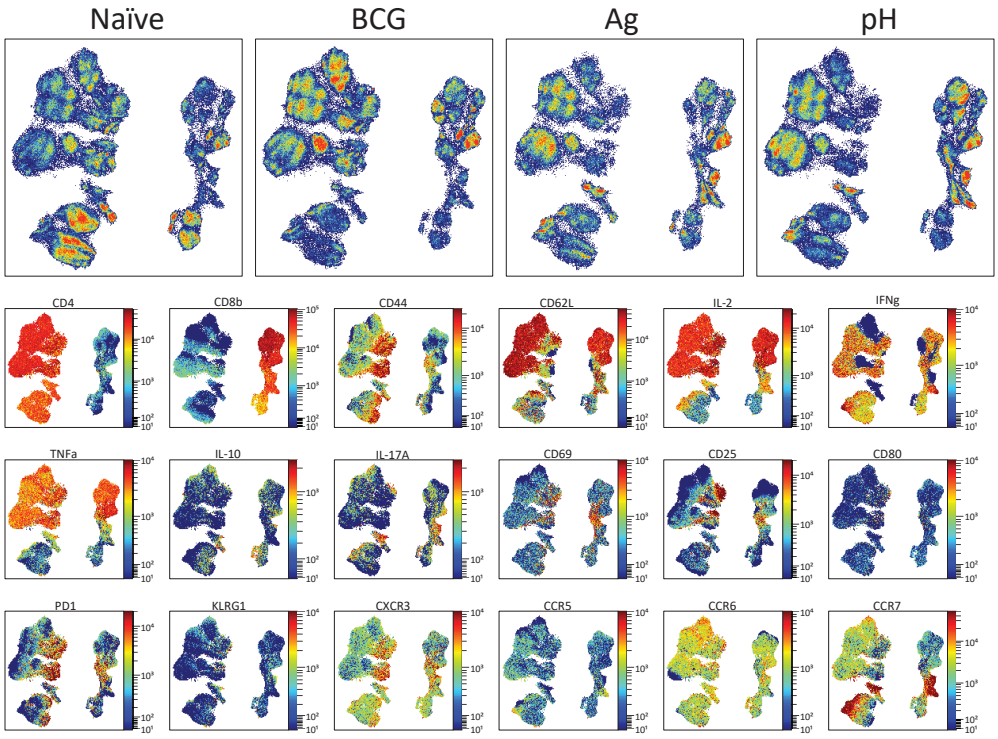

Figure 2. Uniform Manifold Approximation and Projection for Dimension Reduction (UMAP) visualization of spleen-derived CD4⁺, and CD8⁺ T-cells (CD3⁺ CD19⁻) from all tested mice (per group) showing differential abundances of various populations of cells followed by color-continuous plots depicting phenotypical markers distribution. Groups represent: naïve – unimmunized mice, BCG – BCG vaccination, Ag – AER/CpG/MPLA mixture vaccination, pH – vaccination with cationic pH-sensitive liposomal formulation of AER/CpG/MPLA.

TNFα⁻ CCR7⁺ T-cells was differentially enriched, being statistically increased both in AER mixed with CpG/MPLA and AER delivered in the liposomal formulation compared to naïve and BCG-vaccinated mice and displayed a predominant effector memory phenotype. Two monofunctional subpopulations of CD4⁺ T-cells that produced IL-2 were increased in mice vaccinated with BCG. CD4⁺ IL-2⁺ IFNγ⁻ TNFα⁻ IL-17A⁻ IL-10⁻ CD44⁻ CD62L⁺ CCR7⁻ T-cells were significantly increased in the BCG group compared to naïve and both subunit vaccine groups. CD4⁺ IL-2⁺ IFNγ⁻ TNFα⁻ CCR7⁺ T-cells were increased in BCG and AER adjuvant mix compared to naïve and AER delivered in the liposomes. We did not observe any increase in IL-17A production by CD4⁺ T cells followed by any of the immunization.

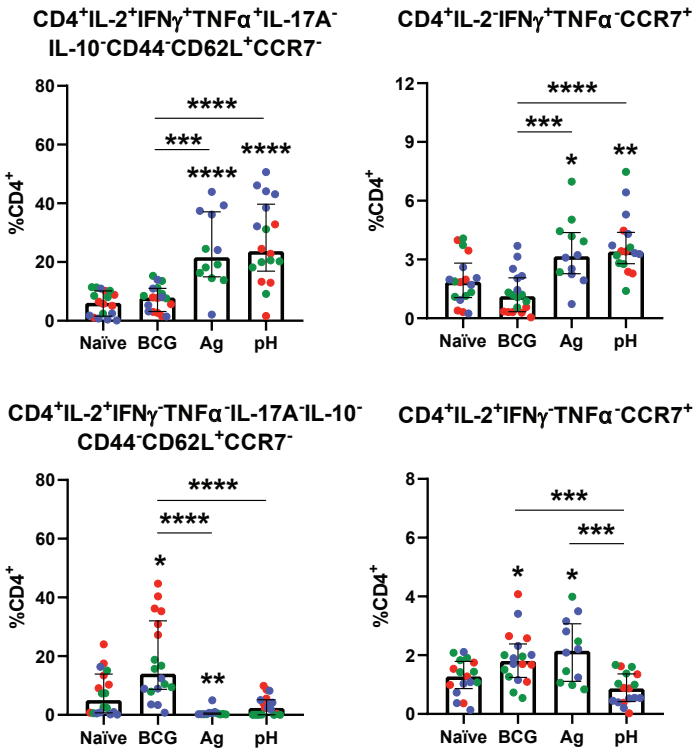

Figure 3. Differentially abundant populations of CD4⁺ T-cells present in restimulated splenocytes from immunized non-Mtb-challenged mice. Markers defining each population are indicated above each graph. Graph values depict percentages of the population as a part of the CD3⁺ CD19⁻ CD4⁺ CD8⁻ cell subset. Each dot represents a single mouse and results from the same experiment are shown in one color. Groups represent: naïve – unimmunized mice, BCG – BCG vaccination, Ag – AER/CpG/MPLA mixture vaccination, pH – vaccination with cationic pH-sensitive liposomal formulation of AER/CpG/MPLA. n = 18 (mice) except Ag group – n =12. Median ± IQR.The minimal number of events used in the analysis was 20,000.

3.5 The abundance of several polyfunctional and monofunctional CD8⁺ T-cell populations increased after immunization

We observed several populations of differentially abundant CD8⁺ T-cells, with the largest subset defined as CD8⁺ IL-2⁺ IFNγ⁺ TNFα⁺ CD44⁻ CD62L⁺ CCR7⁻ (Figure 4). These polyfunctional cells were significantly more abundant in mice vaccinated with AER mixed with CpG/MPLA, and AER in pH-sensitive liposomal adjuvant compared to naïve and BCG-vaccinated mice. We also found a subpopulation that expressed the activation marker CD69 – also known as the activation inducer molecule, a marker of very early activation.[41] This subpopulation

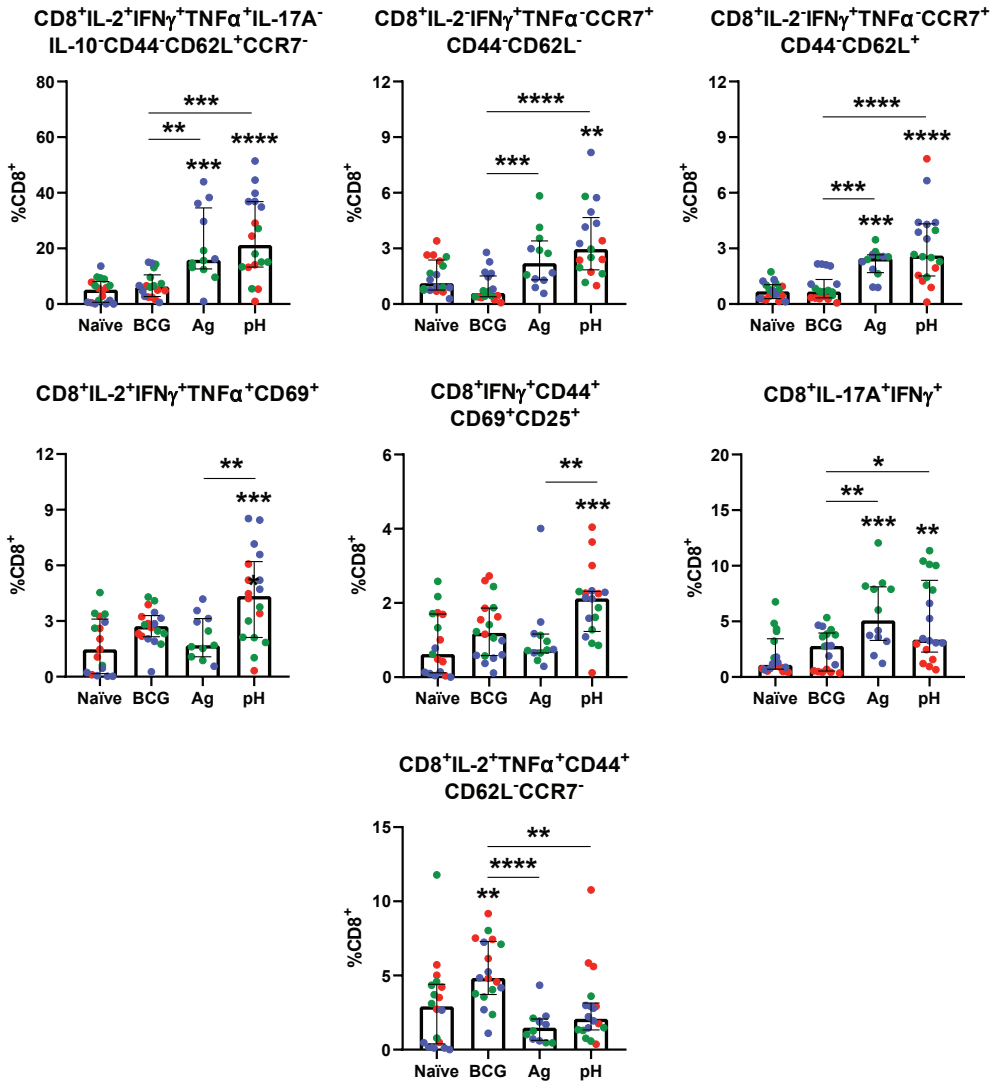

Figure 4. Differentially abundant populations of CD8⁺ T-cells present in restimulated splenocytes from immunized non-Mtb-challenged mice. Markers defining each population are indicated above each graph. Graph values depict percentages of the population as a part of the CD3⁺ CD19⁻ CD4⁻ CD8⁺ cell subset. Each dot represents a percentage value from a single mouse and results from the same experiment are shown in one color. Groups represent: naïve – unimmunized mice, BCG – BCG vaccination, Ag – AER/CpG/MPLA mixture vaccination, pH – vaccination with cationic pH-sensitive liposomal formulation of AER/CpG/MPLA. n = 18 (mice) except Ag group – n =12. Median ± IQR. The minimal number of events used in the analysis was 20,000.

was significantly increased in mice vaccinated with AER in pH-sensitive liposomes compared to naïve mice, and mice vaccinated with AER mixed with CpG/MPLA. We also observed two single functional populations of $CD8^+$ T-cell producing only IFNγ – one expressing CCR7 but not CD44 or CD62L, the other expressing both CCR7 and CD62L but not CD44. Both of these populations were increased after immunization with AER and adjuvant mix, and AER in the pH-sensitive liposomal formulation compared to naïve and BCG groups. $CD8^+$ $IFN\gamma^+$ $CD44^+$ $CD69^+$ $CD25^+$ T-cells were significantly more abundant in the pH-sensitive liposomal formulation group compared to naïve and AER mixed with CpG/MPLA. This population expressed three activation markers, which may imply that IFNγ-producing $CD8^+$ T-cells derived from mice immunized with the liposomal vaccine are more broadly and/or readily activated upon antigen restimulation compared to $CD8^+$ T-cells derived from other groups. Also, the percentage of $CD8^+$ $IL\text{-}17A^+$ $IFN\gamma^+$ T-cells was statistically increased in mice in both AER vaccine arms compared to naïve and BCG groups. The $CD8^+$ $IL\text{-}2^+$ $TNF\alpha^+$ $CD44^+$ $CD62L^-$ $CCR7^-$ population of $CD8^+$ T-cells was more abundant in mice vaccinated with BCG but not with any of the two AER vaccine groups –, which corresponds to activated effector memory phenotype.

3.6 Altered B-cell responses in vaccinated mice

B-cell responses in the concatenated dimensionally reduced data (Figure 5) were visually inspected to determine whether there were differences in the abundance of B-cells in different mice groups. Clear differences in various subsets of cells were observed; therefore, the quantitative analysis used the same approach as in the T-cell data analysis. Several differentially abundant B-cell subsets were identified (Figure 6). Several subpopulations of $CD19^+$ $CD3^-$ cells that expressed the activation marker CD69 were observed: $MHCII^+$ IgM^+ IgD^- $B220^+$ (marginal zone B-cell, transitional 1 B), $MHCII^+$ IgM^+ IgD^+ $B220^+$ (transitional 2B, activated B), $MHCII^+$ IgM^- IgD^- $B220^+$ (germinal center B-cell) and $MHCII^+$ IgM^- IgD^+ $B220^+$ (follicular B/B2).[42,43] The percentages of all these subsets were significantly increased in mice immunized with AER in pH-sensitive liposome formulation, and AER mixed with CpG/MPLA compared to naïve and BCG-immunized mice. A population of B cells defined as $MHCII^-$ IgM^+ IgD^- $B220^-$ was observed which could be a transient subpopulation of plasma cells since it did not express CD138. Also, three subsets of $CD19^+$ $CD3^-$ cells that were significantly more abundant in mice vaccinated with BCG but not with AER

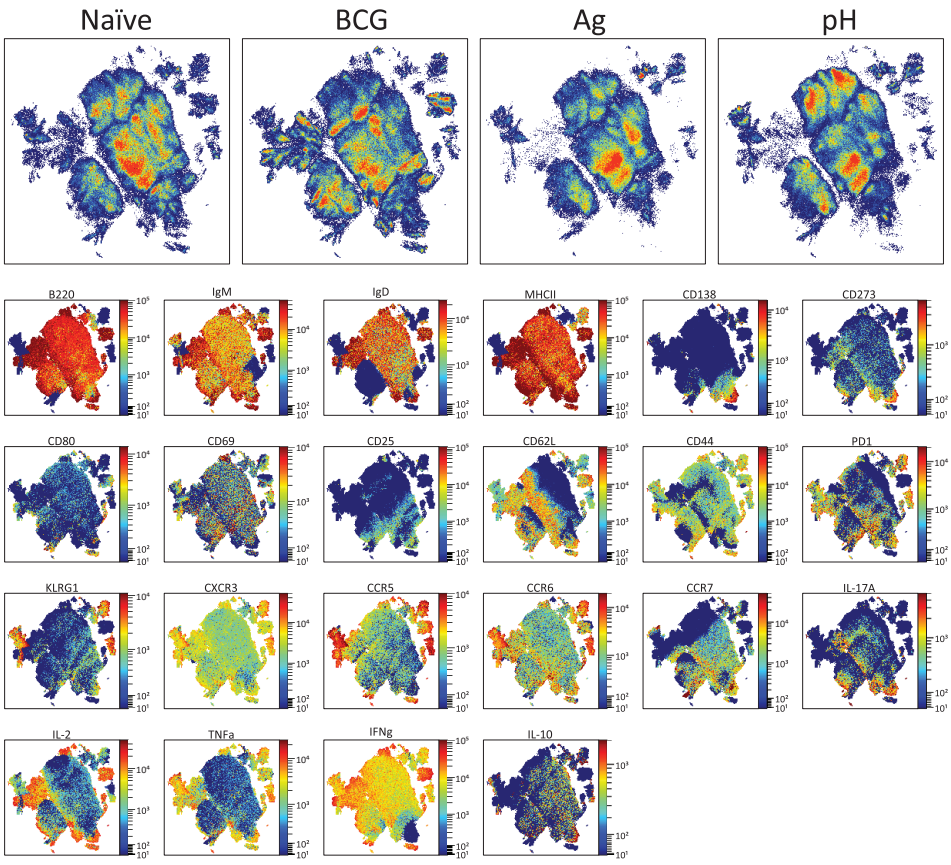

Figure 5. Uniform Manifold Approximation and Projection for Dimension Reduction (UMAP) visualization of concatenated spleen-derived B-cells ($CD3^-$ $CD19^+$) from all tested mice (per group) showing differential abundances of various populations of cells followed by color-continuous plots depicting phenotypical markers distribution. Groups represent: naïve – unimmunized mice, BCG – BCG vaccination, Ag – AER/CpG/MPLA mixture vaccination, pH – vaccination with cationic pH-sensitive liposomal formulation of AER/CpG/MPLA.

CpG/MPLA mix or AER in pH-sensitive liposomes were observed: $CD69^+$ $TNF\alpha^+$ cells $MHCII^+$ $B220^+$ $CD62L^+$ $IL\text{-}17A^+$, and $MHCII^+$ $B220^+$ $CXCR3^+$ $PD\text{-}1^+$.

3.7 High AER-specific antibody titers in vaccinated mice

AER-specific antibody titers in sera of non-Mtb-challenged mice were measured (Figure 7). High total antibody titers and high titers for antibody subclasses were observed: high levels of IgG1, IgG2a, (and IgG2b, IgG2c, and intermediate levels of IgG3 and IgM, Fig S8). Mice vaccinated with AER delivered in pH-sensitive liposomal

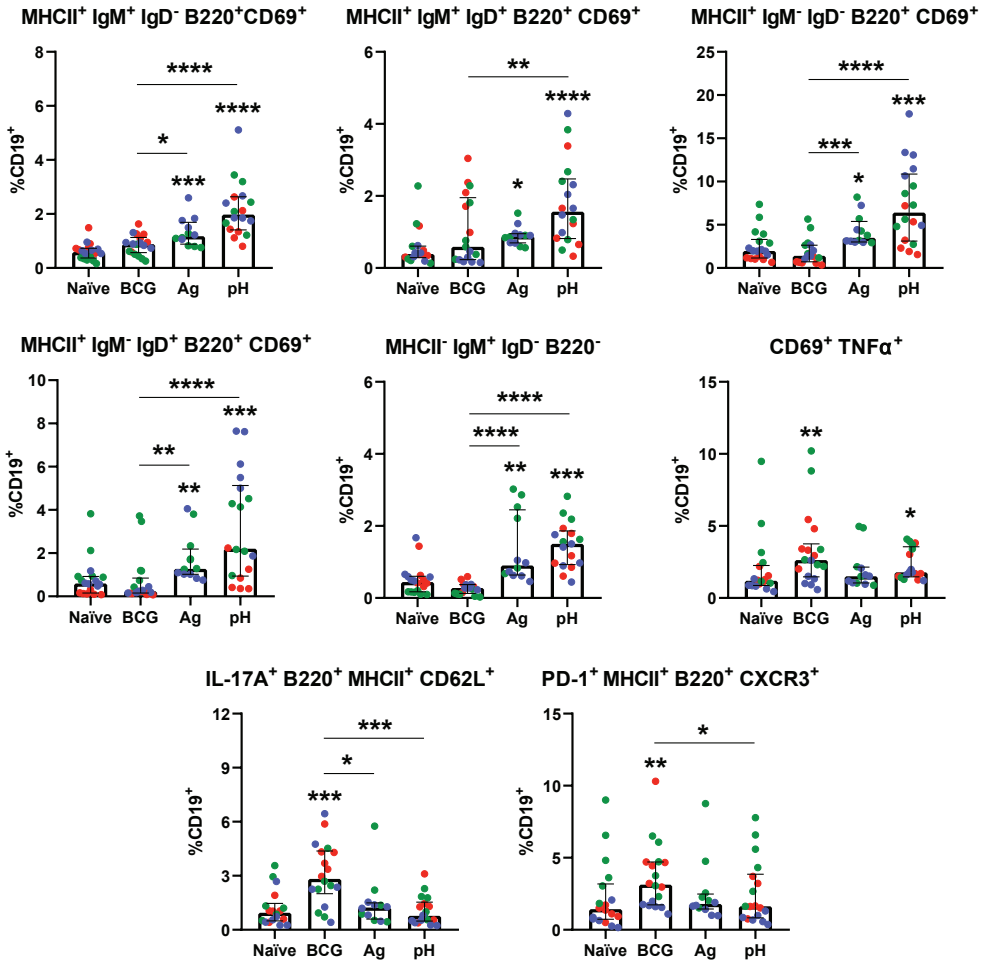

Figure 6. Differentially abundant CD19⁺ B-cell populations present in restimulated splenocytes from immunized non-Mtb-challenged mice. Markers defining each population are indicated above each graph. Graph values depict percentages of the population as a part of the CD3⁻ CD19⁺ cell subset. Each dot represents a percentage value from a single mouse and results from the same experiment are shown in one color. Groups represent: naïve – unimmunized mice, BCG – BCG vaccination, Ag – AER/CpG/MPLA mixture vaccination, pH – vaccination with cationic pH-sensitive liposomal formulation of AER/CpG/MPLA. n = 18 (mice) except Ag group – n =12. Median ± IQR. The minimal number of events used in the analysis was 20,000.

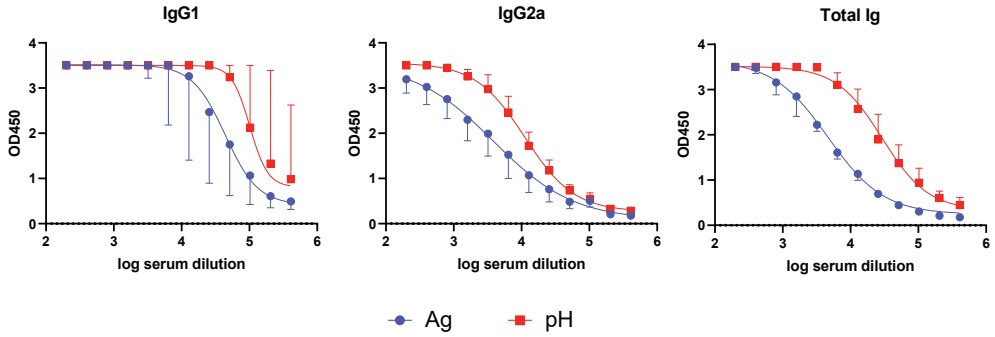

Figure 7. Quantification of serum antibodies to AER. The type of antibody measured is indicated above each graph. Values represent end-point titers. Values of 6 mice. Median ± IQR. ND – titer below detection level.

formulation had higher antibody titers compared to mice immunized with AER mixed with adjuvants. When comparing titers of IgG1 and IgG2a subsets, we observed that the IgG1 titer was higher. Although this might suggest that the balance of immune responses was potentially skewed towards Th2; however, this was not substantiated by the above direct splenocyte T-cell data, where we did not observe any increase in the production of Th2 cytokine IL-10.

4. DISCUSSION

TB for centuries has remained at the top of the deadliest infectious diseases worldwide. One of the reasons why TB poses an immense burden is BCG's variable and incomplete protection against contagious pulmonary TB in adolescents and adults. Despite decades of research, there is no other TB vaccine approved. In this work, we investigated a pH-sensitive liposome-based subunit vaccine that incorporates a triple fusion antigen AER together with two molecular adjuvants CpG and MPLA. pH-sensitive liposomes are a unique class of liposomes that respond to changes in pH in the microenvironment, which has many applications, notably allowing endosomal escape and intracellular delivery of antigens. To the best of our knowledge, this is the first report on the application of pH-sensitive liposomes for protein-based antigen delivery for TB vaccination. In this study, we explored the effectiveness of such a vaccine and whether pH-sensitive liposomes are suitable for further TB vaccine development.

Protection is the main goal of prophylactic vaccination. AER antigen was previously studied by Commandeur et al. and showed the protective effects of a 25 µg AER mixed with CAF09 adjuvant in HLA-DR3 transgenic mice (C57BL/10 background). In

this study, vaccination with AER encapsulated in a DOPC:DOPE:DOBAQ:EPC/MPLA/CpG adjuvant significantly reduced a bacterial load in lungs and spleens of Mtb-infected mice. This vaccine was also more effective than 25 μg AER solution mixed with 50 μg CpG and 1 μg MPLA.

Th1 cells, particularly $CD4^+$ T-cells, play a critical role in immunity against Mtb by producing cytokines and mediating immune responses.[5,44–46] The hallmark cytokine IFNγ is involved in macrophage activation, $CD8^+$ T-cell differentiation, and B-cell activation,[47,48] while TNFα acts synergistically with IFNγ to induce reactive nitrogen species in macrophages, promotes immune cell migration, and modulates granuloma formation.[49] These roles are substantiated by observations of increased susceptibility to BCG infection in infants with IFNγ receptor gene mutations[50] and higher TB reactivation risk in individuals taking TNFα antagonists.[51] IL-2, produced by activated T-cells, stimulates lymphocyte differentiation and proliferation, enhancing cellular immunity,[52] and its low-dose therapy can improve TB symptoms.[53] Vaccination studies in mice[54–56] and humans[57] support the notion of the superior role of polyfunctional T-cells secreting IL-2, TNFα, and IFNγ.[58,59] However, contradicting data question their protective role in TB,[60–63] as well as the association of IFNγ production with vaccine-induced TB protection and Mtb killing.[64–66]

Our data showed higher polyfunctional $CD4^+$ T-cell counts in mice vaccinated with AER mixed with CpG and MPLA, and AER in a pH-sensitive liposomal formulation compared to naïve and BCG-vaccinated mice. These prevalent T-cells expressed CD62L but not CD44 or CCR7, suggesting they may represent a distinct central memory T-cell subset that has shed CD44[67] Such cells were reported to display significant expansion and conferred excellent protection when transferred to $Rag^{-/-}$ mice exposed to Mtb H37Rv aerosol but this was not observed for $CD4^+$ $CD44^{hi}$ $CD62L^{lo}$ cells.[68] $CD4^+$ $CD44^{lo}$ $CD62L^{hi}$ cells likely represent a crucial cell reservoir capable of inducing protection, consistent with a central memory phenotype. We also noted an increase in single functional $IFN\gamma^+$ $CD4^+$ T-cells expressing CCR7, hinting at another central memory subset.[67] In contrast, $CD4^+$ $IL\text{-}2^+$ $IFN\gamma^-$ $TNF\alpha^-$ $CCR7^+$ T-cells were increased by BCG and AER mix, but not by the liposomal vaccine.

Th17 cells, $CD4^+$ T-cells that produce IL-17, play a significant role in the early stages of Mtb protection by recruiting neutrophils and Th1 cells to infection sites, facilitating the formation of mature granuloma and protection.[5,44–46] Despite their contribution

to the initial response in high-dose aerosol Mtb-infected mice,[69] the efficacy of Th17 cells in Mtb protection is disputed. IL-17 deficient or receptor-deficient mice can control Mtb comparably to normal mice, and Th17 responses may not provide adequate protection,[70] and potentially contribute to worsening lung pathology.[71–73] In our data, no increase in Th17 cells was observed following any tested vaccines.

Cytotoxic $CD8^+$ T-cells play a role in protection against Mtb; however, their role is debated. Apart from their main biological function of directly killing infected cells, they also can produce cytokines, modulate host immune response, and work synergistically with Th1 cells.[47,74] It has been proposed that $CD8^+$ T-cells next to Th1 cells are an interesting target for new vaccines against Mtb.[5,75,76] This view is supported by numerous mice studies showing that depletion of $CD8^+$ T-cells using antibodies increased susceptibility to Mtb,[77,78] and genetic knockout experiments demonstrated that they are necessary for the Mtb control.[79–82] In latency, depletion of $CD8^+$ but not $CD4^+$ T-cells resulted in an increase in bacterial burden, signifying their critical role in chronic phases of infection in mice [83] and in non-human primates.[84]

In this study, we observed increased counts of $CD8^+$ T-cells and several populations of polyfunctional cells compared to naïve and BCG-vaccinated mice. The largest population observed was a polyfunctional $CD8^+$ T-cell population that displayed a central memory phenotype similar to that observed in the $CD4^+$ T-cell arm. We also found a subpopulation of these cells that expressed the CD69 marker, which suggests that a fraction of these cells is readily activated upon AER restimulation. Noteworthy, we observed increased IL-17A-producing $CD8^+$ T-cells. It is believed that such cells (Tc17) play a similar role to Th17 cells;[85,86] however, more research is needed to determine their contribution to immune responses against Mtb infection.

B-cell and antibody responses play a role in tuberculosis (TB) immunity, though this is not fully clear yet.[59,87] B-cells may help combat TB through various strategies such as cytokine production, MHC class II antigen presentation, immune regulation and Mtb neutralization, to mention a few.[87] Evidence supporting B-cell involvement includes the high numbers of B-cells in infected lung tissues in mice, non-human primates, and humans,[88,89] heightened susceptibility to Mtb infection in B-cell-depleted mice and non-human primates, resolved after B-cell transfer,[90–92] and B-cell dysfunction

associated with active TB in humans, which normalized after effective treatment.[93] However, this theory faces opposition from genetic knockout results,[90,92,94–99] and different Mtb infection models showing insignificant effects.[97–99]

In our current work, we observed increased subsets of B-cells in splenocyte cultures from mice vaccinated with AER mixed with CpG and MPLA, and the vaccine delivered in a pH-sensitive liposome. These subsets expressed activation marker CD69. We also observed subpopulations of B-cells producing TNFα, and IL-17A. B-cells were shown to influence the expansion and differentiation of Th1[100] and Th2 cells[101] through TNFα production. A study by Deepe et al. demonstrated $CD4^+$ T-cells' inability to clear *Pneumocystis murina* infection without B-cell-derived TNF.[102] B-cells producing IL-17 in response to *Trypanosoma cruzi*, were shown to be important in protection against this parasitic infection.[103] The main IL-17 producers were IgM^+ $CD138^+$ plasmablasts in early infection stages, and were necessary for infection control.[103] IL-17A-producing B-cells could play a crucial role in initial Mtb infection control, which could be further explored in future studies.

Antibodies (Abs) are suggested to contribute to protection against TB. This view is supported by successful serum therapy in Mtb-infected severe combined immunodeficient mice[104] and reduced Mtb burden through high-dose intravenous immunoglobulin in C57Bl/6 mice[105] Transfers of sera from LTBI patients and highly exposed but uninfected individuals also demonstrated protection in mice.[106] Furthermore, monoclonal Abs against specific mycobacterial antigens extended survival,[107,108] limited dissemination,[109] diminished tissue pathology,[110] and decreased mycobacterial burden.[107,110–112] In this study, we observed high total AER-specific Ig titers, as well as subtypes: IgG1, IgG2a, IgG2b, and IgG2c, and intermediate levels of IgG3 and IgM. Mice immunized with AER delivered in pH-sensitive liposomes induced higher antibody titers compared to AER mixed with CpG and MPLA, correlating with the stronger protection afforded by the liposomal vaccine. However, this difference was not statistically significant.

Our study investigated a new tuberculosis subunit vaccine's efficacy, using pH-sensitive liposomes to deliver the AER antigen. We found that it triggered protection in Mtb-challenged C57Bl/6 mice, and induced various immune responses in vaccinated mice, including differentially abundant polyfunctional T- and B-cells, and increased antigen-specific antibody titers. We discovered similar immune responses

using both AER antigen mixed with adjuvants and AER in pH-sensitive liposomes and the latter provided significantly improved protection. Notably, pH-sensitive liposome formulation used three times lower dose of antigen and twenty times lower dose of CpG indicating a significant benefit of using this vaccine delivery system. However, the protection mechanism remains unknown.

The study's key limitation is its single time point assessment, which limits the evaluation of the time-dynamic immune responses and potentially overlooks late or long-term protective effects. In future research, multiple time points should be assessed. The 7-day restimulation of lymphocytes protocol prohibited the study of early immune responses. Our study's reliance on single doses of antigen and liposome restricted understanding of dose-response relationships, and future research should explore varying doses. Likewise, the arbitrary choice and dose of adjuvants may have missed dose-dependent or adjuvant-specific effects. The main strength of this work is the connection of primary human innate responses with adaptive immune responses observed in vaccinated mice, which sheds light on the possibilities of expanding this research to other animal models and translation into human use.

5. CONCLUSIONS

In this research, a novel subunit vaccine was developed targeting TB, which remains at the top of infectious killers globally. The formulation consisted of the Ag85B-ESAT6-Rv2034 fusion antigen, two adjuvants (CpG and MPLA), and a cationic pH-sensitive liposome DOPC:DOPE:DOBAQ:EPC 3:5:2:4 as a delivery system. One of the key contributions of this study is the introduction of pH-sensitive liposomes as a delivery system for TB vaccines, which had not been previously reported. *In vivo* experiments demonstrated that the new vaccine led to a substantial reduction in Mtb bacterial load in the lungs and spleens, outperforming the results observed in mice vaccinated with the antigen mixed with adjuvants but lacking the liposome delivery system. Furthermore, the vaccine induced potent polyfunctional $CD4^+$ and $CD8^+$ T-cell responses. An increase in $CD69^+$ B-cell subpopulations was also observed. In addition to cellular responses, the vaccine stimulated robust antigen-specific antibody titers. Overall, these findings offer new insights into the application of pH-

sensitive liposomes for subunit vaccines against TB. The effectiveness of the vaccine in inducing diverse immune responses underscores its potential as an interesting candidate for future TB vaccine research.

ABBREVIATIONS

AER, Ag85B-ESAT6-Rv2034 antigen; APC, antigen-presenting cell; Ag, antigen(-adjuvant mix group); BCG, Mycobacterium bovis Bacillus Calmette–Guérin; CAF09, cationic adjuvant formulation 09;CCL, chemokine (C-C motif) ligand; CCR, C-C chemokine receptor type; CD, cluster of differentiation; CFU, colony forming unit; CpG ODN, cytosine-phosphorothioate-guanine oligodeoxynucleotides; CXCL, chemokine (C-X-C motif) ligand; CXCR, C-X-C motif chemokine receptor; DC, dendritic cell; DOBAQ, N-(4-carboxybenzyl)-N,N-dimethyl-2,3-bis(oleoyloxy) propan-1-aminium; DOPC, 1,2-dioleoyl-sn-glycero-3-phosphocholine; DOPE, 1,2-dioleoyl-sn-glycero-3-phosphoethanolamine; EPC, 1,2-dioleoyl-sn-glycero-3-ethylphosphocholine; FBS, fetal bovine serum; FDR, false discovery rate; GM-CSF, granulocyte-macrophage colony-stimulating factor; HLA, human leukocyte antigen; HRP, horse radish peroxide; IFN, interferon; Ig, immunoglobulin, IL, interleukin; i.n., intranasal; IQR, interquartile range; KLRG1, killer cell lectin-like receptor subfamily G member 1; MACS, magnetic cell isolation; M-CSF, macrophage colony-stimulating factor; LAL, limulus amebocyte lysate; LUMC, Leiden University Medical Center; MDDC, monocyte-derived dendritic cell; MHC, major histocompatibility complex; MPLA, monophosphoryl lipid A; Mtb, mycobacterium tuberculosis; PAMP, pathogen-associated molecular pattern; PBMC, peripheral blood mononuclear cell; PCR, polymerase chain reaction; PD-1, programmed cell death protein 1; PDI, polydispersity index; PE, phosphatidylethanolamine; pH, pH-sensitive liposome group; rpm, rounds per minute; s.c., subcutaneous; TB, tuberculosis; Th1/Th2/Th17, type 1/2/17 helper T-cell; TLR, Toll-like receptor; TNF, tumor necrosis factor; UMAP, uniform manifold approximation and projection.

APPENDICES

Supplementary materials

CREDIT AUTHOR STATEMENT

M.M. Szachniewicz: Conceptualization, Methodology, Formal Analysis, Investigation, Writing – Original Draft. **S.J.F. van den Eeden**: Conceptualization, Methodology, Investigation, Writing – Original Draft. **K.E. van Meijgaarden**: Conceptualization, Methodology, Writing – Review & Editing, Supervision. **K.L.M.C. Franken**: Methodology, Investigation, Resources. **S. van Veen**: Methodology, Formal Analysis. **A. Geluk**: Conceptualization, Writing – Review & Editing, Project Administration, Funding Acquisition, Supervision. **J.A. Bouwstra**: Conceptualization, Writing – Review & Editing, Project Administration, Funding Acquisition, Supervision. T**.H.M. Ottenhoff**: Conceptualization, Writing – Review & Editing, Project Administration, Funding Acquisition, Primary supervision.

FUNDING

This work was supported by the Dutch Research Council (NWO) Domain Applied and Engineering Sciences grant, project number: 15240.

DECLARATIONS OF INTEREST

None.

REFERENCES

1. World Health Organization. *Global Tuberculosis Report 2022*. (2022).
2. World Health Organization. *Global Tuberculosis Report 2023*. (2023).
3. World Health Organization. The end TB strategy. (2015).
4. Brewer, T. F. Preventing Tuberculosis with Bacillus Calmette-Guérin Vaccine: A Meta-Analysis of the Literature. *Clinical Infectious Diseases* 31, S64–S67 (2000).
5. Ottenhoff, T. H. M. & Kaufmann, S. H. E. Vaccines against Tuberculosis: Where Are We and Where Do We Need to Go? *PLoS Pathogens* 8, e1002607 (2012).
6. Fatima, S. *et al.* Tuberculosis vaccine: A journey from BCG to present. *Life Sciences* 252, 117594 (2020).
7. Andersen, P. & Scriba, T. J. Moving tuberculosis vaccines from theory to practice. *Nature Reviews Immunology* 19:9, 550–562 (2019).
8. Christensen, D. *et al.* Cationic liposomes as vaccine adjuvants. *Expert Review of Vaccines* 10, 513–521 (2011).

9. Liu, X. *et al.* A novel liposome adjuvant DPC mediates Mycobacterium tuberculosis subunit vaccine well to induce cell-mediated immunity and high protective efficacy in mice. *Vaccine* 34, 1370–1378 (2016).
10. Inglut, C. T. *et al.* Immunological and Toxicological Considerations for the Design of Liposomes. *Nanomaterials* 10:2, 190 (2020).
11. Shah, S. *et al.* Liposomes: Advancements and innovation in the manufacturing process. *Advanced Drug Delivery Reviews* 154, 102–122 (2020).
12. Bozzuto, G. & Molinari, A. Liposomes as nanomedical devices. *International Journal of Nanomedicine* 10, 975 (2015).
13. Karanth, H. & Murthy, R. S. R. pH-Sensitive liposomes-principle and application in cancer therapy. *Journal of Pharmacy and Pharmacology* 59, 469–483 (2007).
14. Momekova, D. *et al.* Long-Circulating, pH-Sensitive Liposomes. *Methods in Molecular Biology* 1522, 209–226 (2017).
15. Mu, Y. *et al.* Advances in pH-responsive drug delivery systems. *OpenNano* 5, 100031 (2021).
16. Balamurali, V. *et al.* pH Sensitive Drug Delivery Systems: A Review. *American Journal of Drug Discovery and Development* 1, 24–48 (2010).
17. Fehres, C. M. *et al.* Understanding the biology of antigen cross-presentation for the design of vaccines against cancer. *Frontiers in Immunology* 5, 149 (2014).
18. Melero, I. *et al.* Therapeutic vaccines for cancer: an overview of clinical trials. *Nature Reviews Clinical Oncology 2014 11:9* 11, 509–524 (2014).
19. Paliwal, S. R. *et al.* A review of mechanistic insight and application of pH-sensitive liposomes in drug delivery. *Drug delivery* 22:3, 231–242 (2015).
20. Liu, X. & Huang, G. Formation strategies, mechanism of intracellular delivery and potential clinical applications of pH-sensitive liposomes. *Asian Journal of Pharmaceutical Sciences* 8, 319–328 (2013).
21. Abri Aghdam, M. *et al.* Recent advances on thermosensitive and pH-sensitive liposomes employed in controlled release. *Journal of Controlled Release* 315, 1–22 (2019).
22. Ferreira, D. D. S. *et al.* pH-sensitive liposomes for drug delivery in cancer treatment. *Therapeutic Delivery* 4, 1099–1123 (2013).
23. Gupta, M. *et al.* pH-sensitive liposomes. *Liposomal Delivery Systems: Advances and Challenges* 1, 74–86 (2015).

24. Commandeur, S. *et al.* Double- and monofunctional CD4+ and CD8+ T-cell responses to Mycobacterium tuberculosis DosR antigens and peptides in long-term latently infected individuals. *European Journal of Immunology* 41, 2925–2936 (2011).
25. Commandeur, S. *et al.* The in vivo expressed Mycobacterium tuberculosis (IVE-TB) antigen Rv2034 induces CD4+ T-cells that protect against pulmonary infection in HLA-DR transgenic mice and guinea pigs. *Vaccine* 32, 3580–3588 (2014).
26. Luabeya, A. K. K. *et al.* First-in-human trial of the post-exposure tuberculosis vaccine H56:IC31 in Mycobacterium tuberculosis infected and non-infected healthy adults. *Vaccine* 33, 4130–4140 (2015).
27. Commandeur, S. *et al.* An Unbiased Genome-Wide Mycobacterium tuberculosis Gene Expression Approach To Discover Antigens Targeted by Human T Cells Expressed during Pulmonary Infection. *The Journal of Immunology* 190, 1659–1671 (2013).
28. Ko, E. J. *et al.* MPL and CpG combination adjuvants promote homologous and heterosubtypic cross protection of inactivated split influenza virus vaccine. *Antiviral Research* 156, 107–115 (2018).
29. Todoroff, J. *et al.* Mucosal and Systemic Immune Responses to Mycobacterium tuberculosis Antigen 85A following Its Co-Delivery with CpG, MPLA or LTB to the Lungs in Mice. *PLoS One* 8, e63344 (2013).
30. Meraz, I. M. *et al.* Adjuvant cationic liposomes presenting MPL and IL-12 induce cell death, suppress tumor growth, and alter the cellular phenotype of tumors in a murine model of breast cancer. *Molecular Pharmaceutics* 11, 3484–3491 (2014).
31. Kruit, W. H. J. *et al.* Selection of immunostimulant AS15 for active immunization with MAGE-A3 protein: results of a randomized phase II study of the European Organisation for Research and Treatment of Cancer Melanoma Group in Metastatic Melanoma. *Journal of Clinical Oncology* 31, 2413–2420 (2013).
32. Vansteenkiste, J. F. *et al.* Efficacy of the MAGE-A3 cancer immunotherapeutic as adjuvant therapy in patients with resected MAGE-A3-positive non-small-cell lung cancer (MAGRIT): a randomised, double-blind, placebo-controlled, phase 3 trial. *Lancet Oncology* 17, 822–835 (2016).

33. Dreno, B. *et al.* MAGE-A3 immunotherapeutic as adjuvant therapy for patients with resected, MAGE-A3-positive, stage III melanoma (DERMA): a double-blind, randomised, placebo-controlled, phase 3 trial. *Lancet Oncology* 19, 916–929 (2018).
34. Kruit, W. H. *et al.* Immunization with recombinant MAGE-A3 protein combined with adjuvant systems AS15 or AS02B in patients with unresectable and progressive metastatic cutaneous melanoma: A randomized open-label phase II study of the EORTC Melanoma Group (16032- 18031). *Journal of Clinical Oncology* 26, 9065–9065 (2008).
35. Gutzmer, R. *et al.* Safety and immunogenicity of the PRAME cancer immunotherapeutic in metastatic melanoma: results of a phase I dose escalation study. *ESMO Open* 1, e000068 (2016).
36. Franken, K. L. M. C. *et al.* Purification of His-Tagged Proteins by Immobilized Chelate Affinity Chromatography: The Benefits from the Use of Organic Solvent. *Protein Expression and Purification* 18, 95–99 (2000).
37. Szachniewicz, M. M. *et al.* Intrinsic immunogenicity of liposomes for tuberculosis vaccines: effect of cationic lipid and cholesterol. *European Journal of Pharmaceutical Sciences* 195, 106730 (2024).
38. Geluk, A. *et al.* A multistage-polyepitope vaccine protects against Mycobacterium tuberculosis infection in HLA-DR3 transgenic mice. *Vaccine* 30, 7513–7521 (2012).
39. R Core Team. R: A language and environment for statistical computing. (2023).
40. RStudio Team. RStudio: Integrated Development Environment for R. (2023).
41. Marzio, R., Mauël, J. & Betz-Corradin, S. CD69 and regulation of the immune function. *Immunopharmacology and Immunotoxicology* 21, 565–582 (1999).
42. Pillai, S. & Cariappa, A. The follicular versus marginal zone B lymphocyte cell fate decision. *Nature Reviews Immunology 2009 9:11* 9, 767–777 (2009).
43. Kleiman, E. *et al.* Distinct transcriptomic features are associated with transitional and mature B-cell populations in the mouse spleen. *Frontiers in Immunology* 6, 126060 (2015).
44. Flynn, J. A. L. Immunology of tuberculosis and implications in vaccine development. *Tuberculosis* 84, 93–101 (2004).
45. Ernst, J. D. The immunological life cycle of tuberculosis. *Nature Reviews Immunology 2012 12:8* 12, 581–591 (2012).

46. Ottenhoff, T. H. M. *et al.* Human CD4 and CD8 T Cell Responses to Mycobacterium tuberculosis: Antigen Specificity, Function, Implications and Applications. *Handbook of Tuberculosis* 119–155 (2008).
47. Prezzemolo, T. *et al.* Functional signatures of human CD4 and CD8 T cell responses to Mycobacterium tuberculosis. *Frontiers in Immunology* 5, 83298 (2014).
48. Tau, G. & Rothman, P. Biologic functions of the IFN-γ receptors. *Allergy* 54, 1233–1251 (1999).
49. Cavalcanti, Y. V. N. *et al.* Role of TNF-alpha, IFN-gamma, and IL-10 in the development of pulmonary tuberculosis. *Pulmonary Medicine* 2012:1, 745483 (2012).
50. Ottenhoff, T. H. M. *et al.* Genetics, cytokines and human infectious disease: lessons from weakly pathogenic mycobacteria and salmonellae. *Nature Genetics 2002 32:1* 32, 97–105 (2002).
51. Toussirot, É. & Wending, D. The use of TNF-α blocking agents in rheumatoid arthritis: an update. *Expert Opinion on Pharmacotherapy* 8, 2089–2107 (2007).
52. Kelso, A. *et al.* Interleukin 2 enhancement of lymphokine secretion by T lymphocytes: analysis of established clones and primary limiting dilution microcultures. *The Journal of Immunology* 132, 2932–2938 (1984).
53. Johnson, B. J. *et al.* Clinical and immune responses of tuberculosis patients treated with low-dose IL-2 and multidrug therapy. *Cytokines and Molecular Therapy* 1, 185–196 (1995).
54. Aagaard, C. *et al.* A multistage tuberculosis vaccine that confers efficient protection before and after exposure. *Nature Medicine* 17:2, 189–194 (2011).
55. Derrick, S. C. *et al.* Vaccine-induced anti-tuberculosis protective immunity in mice correlates with the magnitude and quality of multifunctional CD4 T cells. *Vaccine* 29, 2902–2909 (2011).
56. Lindenstrøm, T. *et al.* Tuberculosis Subunit Vaccination Provides Long-Term Protective Immunity Characterized by Multifunctional CD4 Memory T Cells. *The Journal of Immunology* 182, 8047–8055 (2009).
57. Abel, B. *et al.* The Novel Tuberculosis Vaccine, AERAS-402, Induces Robust and Polyfunctional CD4+ and CD8+ T Cells in Adults. *American Journal of Respiratory and Critical Care Medicine* 181, 1407–1417 (2012).

58. Counoupas, C. *et al.* Deciphering protective immunity against tuberculosis: implications for vaccine development. *Expert Review of Vaccines* 18, 353–364 (2019).
59. Duong, V. T. *et al.* Towards the development of subunit vaccines against tuberculosis: The key role of adjuvant. *Tuberculosis* 139, 102307 (2023).
60. Harari, A. *et al.* Dominant TNF-α+ Mycobacterium tuberculosis–specific CD4+ T cell responses discriminate between latent infection and active disease. *Nature Medicine 2011 17:3* 17, 372–376 (2011).
61. Caccamo, N. *et al.* Multifunctional CD4+ T cells correlate with active Mycobacterium tuberculosis infection. *European Journal of Immunology* 40, 2211–2220 (2010).
62. Sutherland, J. S. *et al.* Pattern and diversity of cytokine production differentiates between Mycobacterium tuberculosis infection and disease. *European Journal of Immunology* 39, 723–729 (2009).
63. Lewinsohn, D. A. *et al.* Polyfunctional CD4+ T cells as targets for tuberculosis vaccination. *Frontiers in Immunology* 8, 295382 (2017).
64. Cowley, S. C. & Elkins, K. L. CD4+ T Cells Mediate IFN-γ-Independent Control of Mycobacterium tuberculosis Infection Both In Vitro and In Vivo. *The Journal of Immunology* 171, 4689–4699 (2003).
65. Gallegos, A. M. *et al.* A Gamma Interferon Independent Mechanism of CD4 T Cell Mediated Control of M. tuberculosis Infection in vivo. *PLoS Pathogens* 7, e1002052 (2011).
66. You, Q. *et al.* Subcutaneous Administration of Modified Vaccinia Virus Ankara Expressing an Ag85B-ESAT6 Fusion Protein, but Not an Adenovirus-Based Vaccine, Protects Mice Against Intravenous Challenge with Mycobacterium tuberculosis. *Scandinavian Journal of Immunology* 75, 77–84 (2012).
67. Henao-Tamayo, M. I. *et al.* Phenotypic definition of effector and memory T-lymphocyte subsets in mice chronically infected with mycobacterium tuberculosis. *Clinical and Vaccine Immunology* 17, 618–625 (2010).
68. Kipnis, A. *et al.* Memory T Lymphocytes Generated by Mycobacterium bovis BCG Vaccination Reside within a CD4 CD44lo CD62 Ligandhi Population. *Infection and Immunity* 73, 7759 (2005).
69. Khader, S. A. *et al.* IL-23 and IL-17 in the establishment of protective pulmonary CD4+ T cell responses after vaccination and during Mycobacterium tuberculosis challenge. *Nature Immunology* 8:4, 369–377 (2007).

70. Ashhurst, A. S. *et al.* PLGA particulate subunit tuberculosis vaccines promote humoral and Th17 responses but do not enhance control of Mycobacterium tuberculosis infection. *PLoS One* 13, e0194620 (2018).
71. Cruz, A. *et al.* Pathological role of interleukin 17 in mice subjected to repeated BCG vaccination after infection with Mycobacterium tuberculosis. *Journal of Experimental Medicine* 207, 1609–1616 (2010).
72. Turner, J. *et al.* Effective preexposure tuberculosis vaccines fail to protect when they are given in an immunotherapeutic mode. *Infection and Immunity* 68, 1706–1709 (2000).
73. Taylor, J. L. *et al.* Pulmonary necrosis resulting from DNA vaccination against tuberculosis. *Infection and Immunity* 71, 2192–2198 (2003).
74. Lu, Y. J. *et al.* CD4 T cell help prevents CD8 T cell exhaustion and promotes control of Mycobacterium tuberculosis infection. *Cell Reports* 36, 109696 (2021).
75. Behar, S. M. *et al.* Next generation: tuberculosis vaccines that elicit protective CD8+ T cells. *Expert Review of Vaccines* 6, 441–456 (2007).
76. Boom, W. H. New TB vaccines: is there a requirement for CD8+ T cells? *Journal of Clinical Investigation* 117, 2092–2094 (2007).
77. Woodworth, J. S. *et al.* Mycobacterium tuberculosis-Specific CD8+ T Cells Require Perforin to Kill Target Cells and Provide Protection In Vivo. *The Journal of Immunology* 181, 8595–8603 (2008).
78. Mogues, T. *et al.* The Relative Importance of T Cell Subsets in Immunity and Immunopathology of Airborne Mycobacterium tuberculosis Infection in Mice. *Journal of Experimental Medicine* 193, 271–280 (2001).
79. Orme, I. M. The kinetics of emergence and loss of mediator T lymphocytes acquired in response to infection with Mycobacterium tuberculosis. *The Journal of Immunology* 138, 293–298 (1987).
80. Flynn, J. L. *et al.* Major histocompatibility complex class I-restricted T cells are required for resistance to Mycobacterium tuberculosis infection. *Proceedings of the National Academy of Sciences* 89, 12013–12017 (1992).
81. Sousa, A. O. *et al.* Relative contributions of distinct MHC class I-dependent cell populations in protection to tuberculosis infection in mice. *Proceedings of the National Academy of Sciences* 97, 4204–4208 (2000).

82. Behar, S. M. *et al.* Susceptibility of Mice Deficient in CD1D or TAP1 to Infection with Mycobacterium tuberculosis. *Journal of Experimental Medicine* 189, 1973–1980 (1999).
83. Van Pinxteren, L. A. H. *et al.* Control of latent Mycobacterium tuberculosis infection is dependent on CD8 T cells. *European Journal of Immunology* 30, 3689–3698 (2000).
84. Lin, P. L. *et al.* CD4 T Cell Depletion Exacerbates Acute Mycobacterium tuberculosis While Reactivation of Latent Infection Is Dependent on Severity of Tissue Depletion in Cynomolgus Macaques. *AIDS Research and Human Retroviruses* 28, 1693–1702 (2012).
85. Mills, K. H. G. IL-17 and IL-17-producing cells in protection versus pathology. *Nature Reviews Immunology 2022 23:1* 23, 38–54 (2022).
86. Ciric, B. *et al.* IL-23 Drives Pathogenic IL-17-Producing CD8+ T Cells. *The Journal of Immunology* 182, 5296–5305 (2009).
87. Rijnink, W. F. *et al.* B-Cells and Antibodies as Contributors to Effector Immune Responses in Tuberculosis. *Frontiers in Immunology* 12, 640168 (2021).
88. Phuah, J. Y. *et al.* Activated B Cells in the Granulomas of Nonhuman Primates Infected with Mycobacterium tuberculosis. *American Journal of Pathology* 181, 508–514 (2012).
89. Tsai, M. C. *et al.* Characterization of the tuberculous granuloma in murine and human lungs: cellular composition and relative tissue oxygen tension. *Cell Microbiology* 8, 218–232 (2006).
90. Maglione, P. J. *et al.* B Cells Moderate Inflammatory Progression and Enhance Bacterial Containment upon Pulmonary Challenge with Mycobacterium tuberculosis. *The Journal of Immunology* 178, 7222–7234 (2007).
91. Phuah, J. *et al.* Effects of B cell depletion on early Mycobacterium tuberculosis infection in cynomolgus macaques. *Infection and Immunity* 84, 1301–1311 (2016).
92. Vordermeier, H. M. *et al.* Increase of tuberculous infection in the organs of B cell-deficient mice. *Clinical & Experimental Immunology* 106, 312–316 (2003).
93. Joosten, S. A. *et al.* Patients with Tuberculosis Have a Dysfunctional Circulating B-Cell Compartment, Which Normalizes following Successful Treatment. *PLoS Pathogens* 12, e1005687 (2016).

94. Khera, A. K. *et al.* Role of B Cells in Mucosal Vaccine–Induced Protective CD8+ T Cell Immunity against Pulmonary Tuberculosis. *The Journal of Immunology* 195, 2900–2907 (2015).
95. Kozakiewicz, L. *et al.* B Cells Regulate Neutrophilia during Mycobacterium tuberculosis Infection and BCG Vaccination by Modulating the Interleukin-17 Response. *PLoS Pathogens* 9, e1003472 (2013).
96. Torrado, E. *et al.* Differential and Site Specific Impact of B Cells in the Protective Immune Response to Mycobacterium tuberculosis in the Mouse. *PLoS One* 8, e61681 (2013).
97. Turner, J. *et al.* The progression of chronic tuberculosis in the mouse does not require the participation of B lymphocytes or interleukin-4. *Experimental Gerontology* 36, 537–545 (2001).
98. Bosio, C. M. *et al.* Infection of B Cell-Deficient Mice with CDC 1551, a Clinical Isolate of Mycobacterium tuberculosis: Delay in Dissemination and Development of Lung Pathology. *The Journal of Immunology* 164, 6417–6425 (2000).
99. Johnson, C. M. *et al.* Mycobacterium tuberculosis aerogenic rechallenge infections in B cell-deficient mice. *Tubercle and Lung Disease* 78, 257–261 (1997).
100. Menard, L. C. *et al.* B Cells Amplify IFN-γ Production By T Cells via a TNF-α-Mediated Mechanism. *The Journal of Immunology* 179, 4857–4866 (2007).
101. Wojciechowski, W. *et al.* Cytokine-Producing Effector B Cells Regulate Type 2 Immunity to H. polygyrus. *Immunity* 30, 421–433 (2009).
102. Opata, M. M. *et al.* B Cell Production of Tumor Necrosis Factor in Response to Pneumocystis murina Infection in Mice. *Infection and Immunity* 81, 4252 (2013).
103. Bermejo, D. A. *et al.* Trypanosoma cruzi trans-sialidase initiates a program independent of the transcription factors RORγt and Ahr that leads to IL-17 production by activated B cells. *Nature Immunology* 14:5, 514–522 (2013).
104. Guirado, E. *et al.* Passive serum therapy with polyclonal antibodies against Mycobacterium tuberculosis protects against post-chemotherapy relapse of tuberculosis infection in SCID mice. *Microbes and Infection* 8, 1252–1259 (2006).

105. Roy, E. *et al.* Therapeutic efficacy of high-dose intravenous immunoglobulin in Mycobacterium tuberculosis infection in mice. *Infection and Immunity* 73, 6101–6109 (2005).
106. Li, H. *et al.* Latently and uninfected healthcare workers exposed to TB make protective antibodies against Mycobacterium tuberculosis. *Proceedings of the National Academy of Sciences of the United States of America* 114, 5023–5028 (2017).
107. Hamasur, B. *et al.* A mycobacterial lipoarabinomannan specific monoclonal antibody and its F(ab')2 fragment prolong survival of mice infected with Mycobacterium tuberculosis. *Clinical & Experimental Immunology* 138, 30–38 (2004).
108. Chambers, M. A. *et al.* Antibody bound to the surface antigen MPB83 of Mycobacterium bovis enhances survival against high dose and low dose challenge. *FEMS Immunology and Medical Microbiology* 41, 93–100 (2004).
109. Pethe, K. *et al.* The heparin-binding haemagglutinin of M. tuberculosis is required for extrapulmonary dissemination. *Nature* 412:6843, 190–194 (2001).
110. López, Y. *et al.* Induction of a protective response with an IgA monoclonal antibody against Mycobacterium tuberculosis 16 kDa protein in a model of progressive pulmonary infection. *International Journal of Medical Microbiology* 299, 447–452 (2009).
111. Zimmermann, N. *et al.* Human isotype-dependent inhibitory antibody responses against Mycobacterium tuberculosis. *EMBO Molecular Medicine* 8, 1325–1339 (2016).
112. Balu, S. *et al.* A Novel Human IgA Monoclonal Antibody Protects against Tuberculosis. *The Journal of Immunology* 186, 3113–3119 (2011).

SUPPLEMENTARY MATERIALS

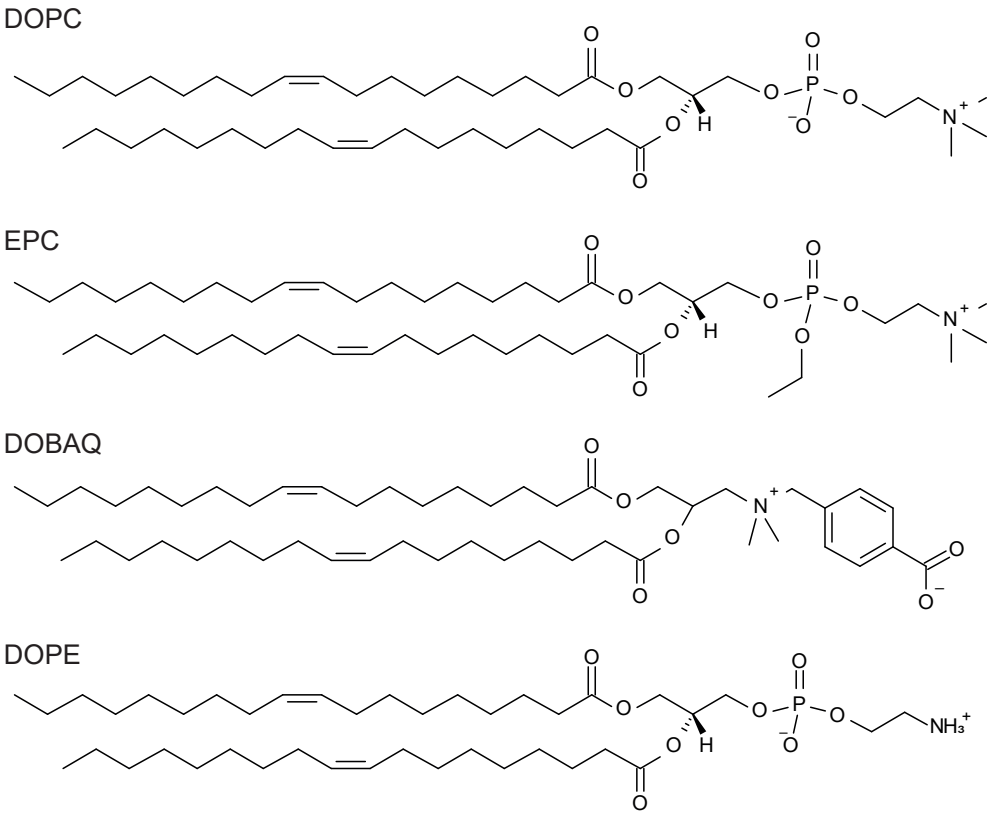

Supplementary Figure S1. Chemical structures of lipids used in the production of pH-sensitive liposomes.

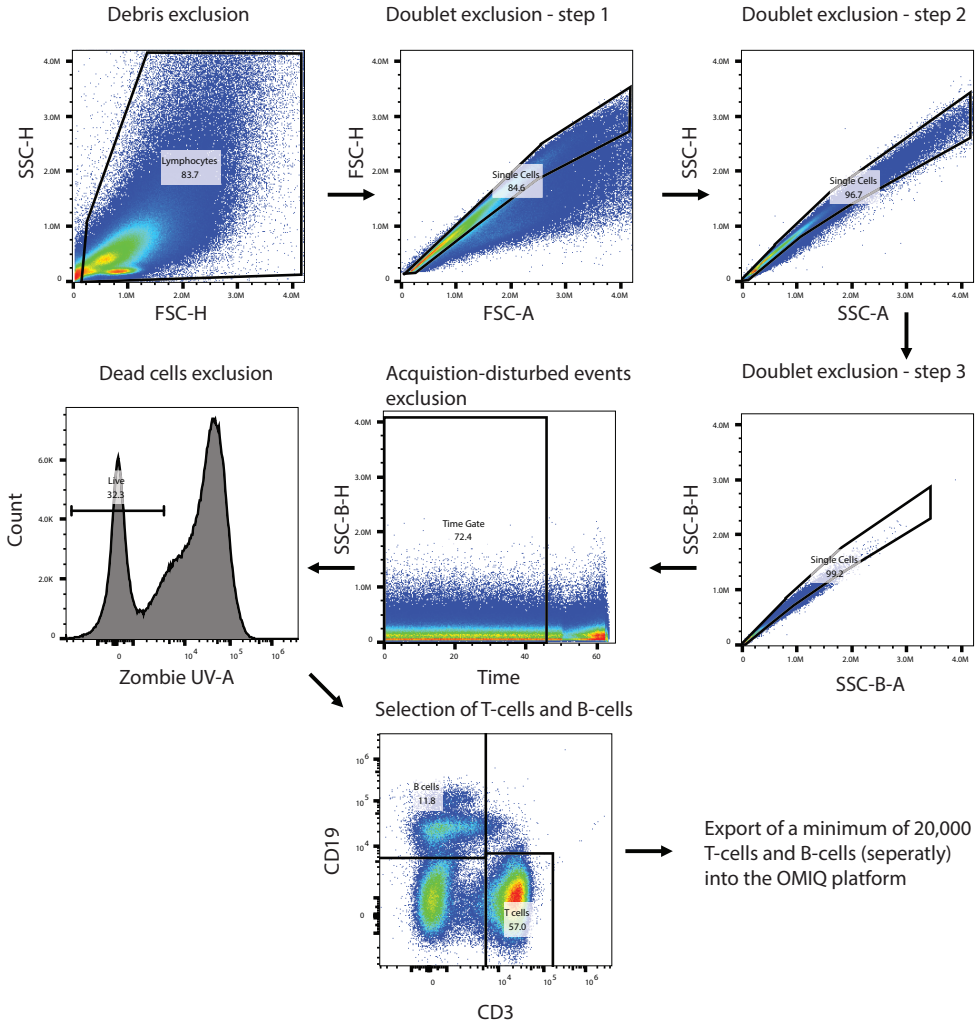

Supplementary Figure S2. Scheme of a gating strategy used to pregate data for further analysis in the OMIQ platform.

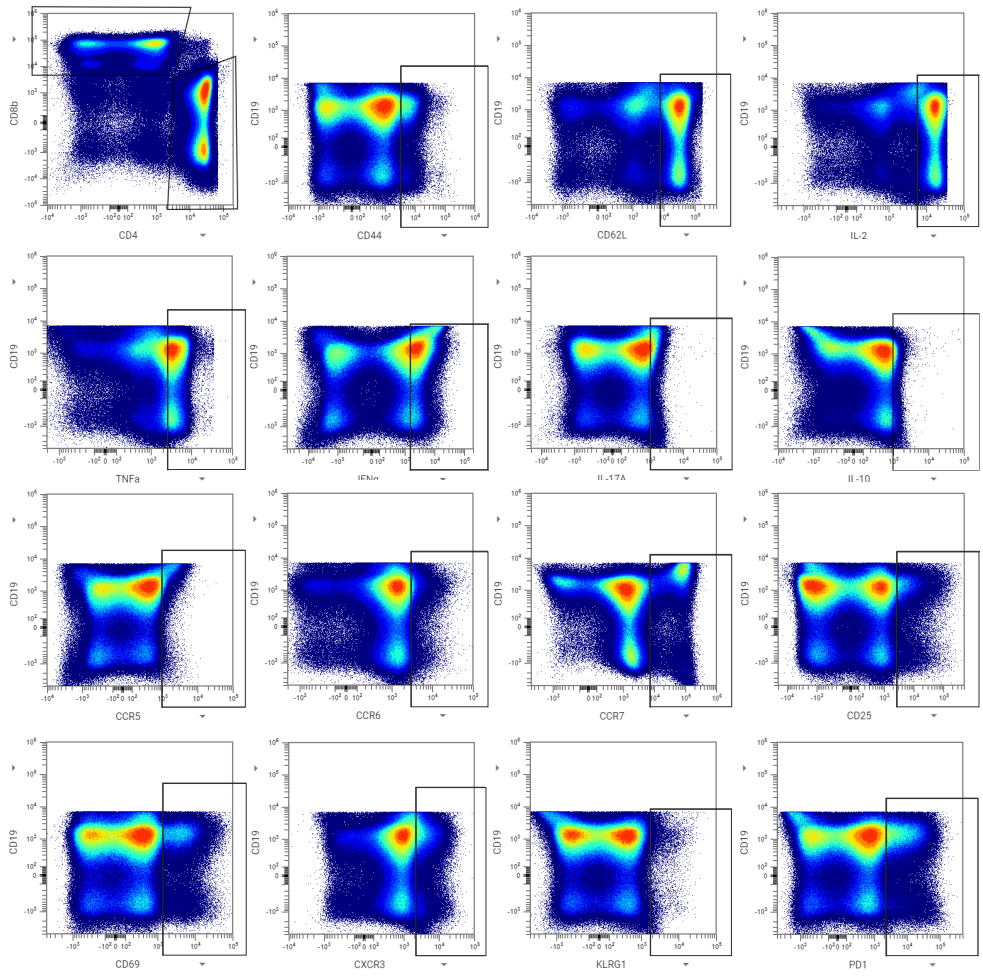

Supplementary Figure S3. Gates used for the creation of Boolean gates for the analysis of T-cell subsets.

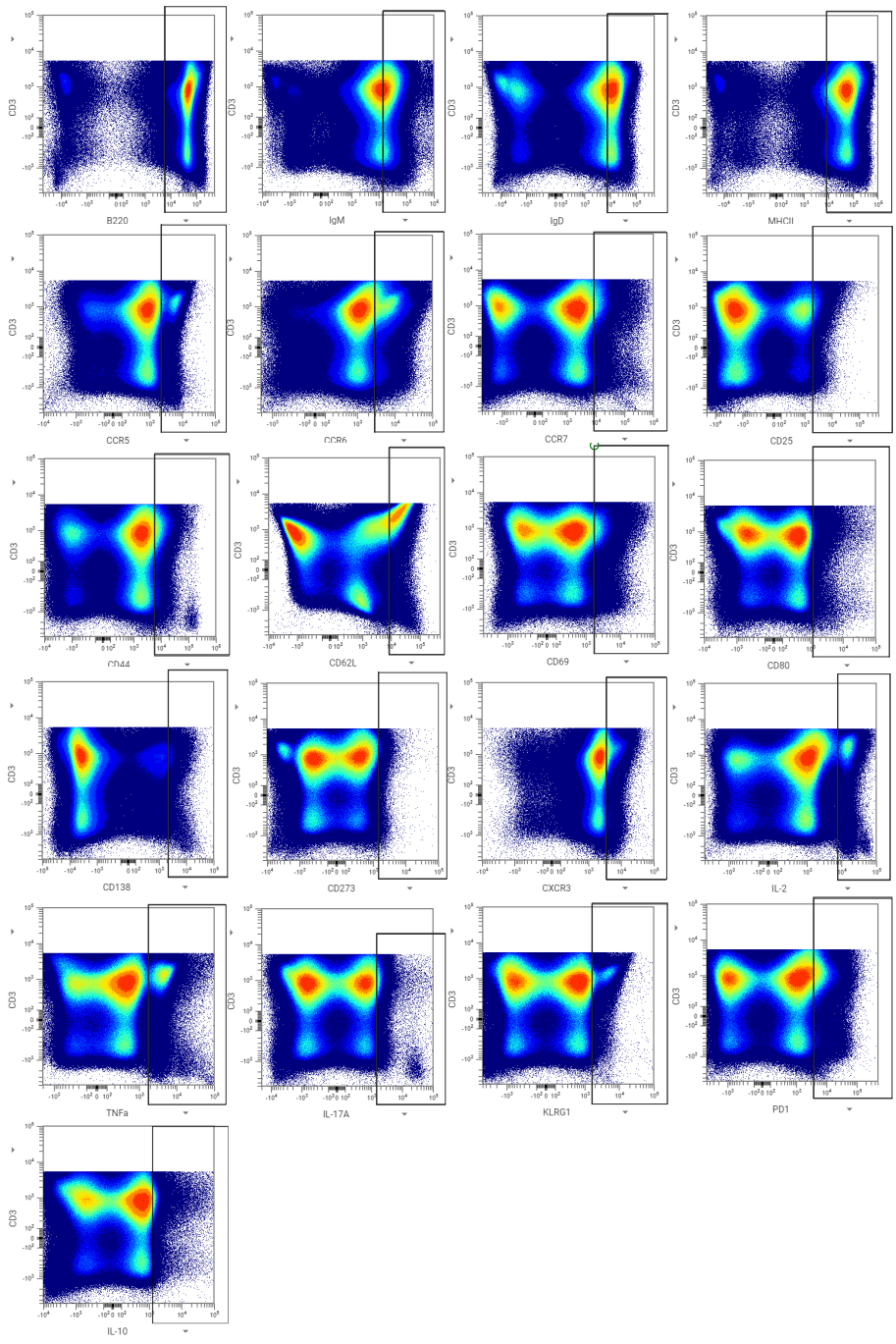

Supplementary Figure S4. Gates used for the creation of Boolean gates for the analysis of B-cell subsets.

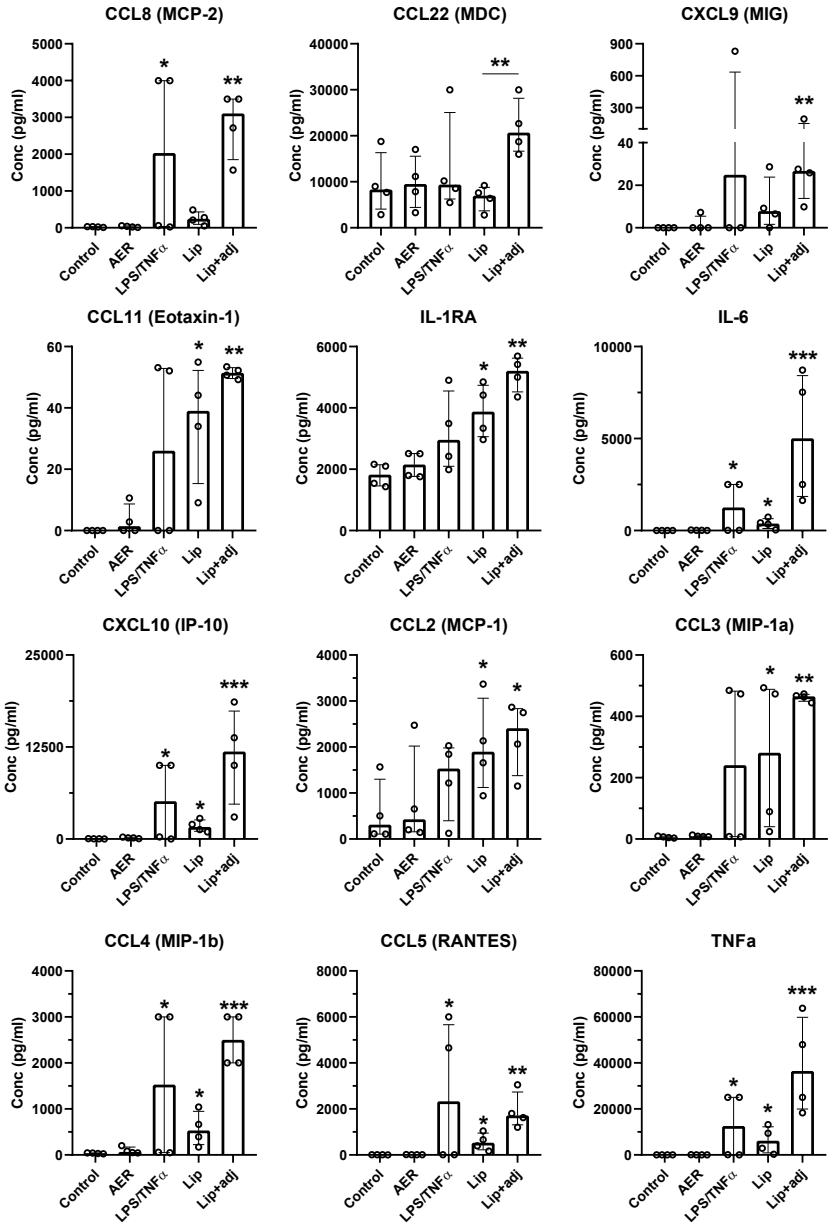

Supplementary Figure S5. Production of cytokines by MDDCs exposed to liposomal formulations (5 µg/ml AER, 250 µg/ml liposomes, exposure 1 h), Lip – unadjuvanted formulation, and Lip+adj – adjuvanted with 12.5 µg/ml CpG, and 5 µg/ml MPLA compared to control (medium only). AER - 5 µg/ml AER, exposure 1 h, LPS/TNFα - 100 and 5 ng/ml respectively, exposure 16 hours (positive control), n = 4 (cell donors). The results represent median ± IQR.

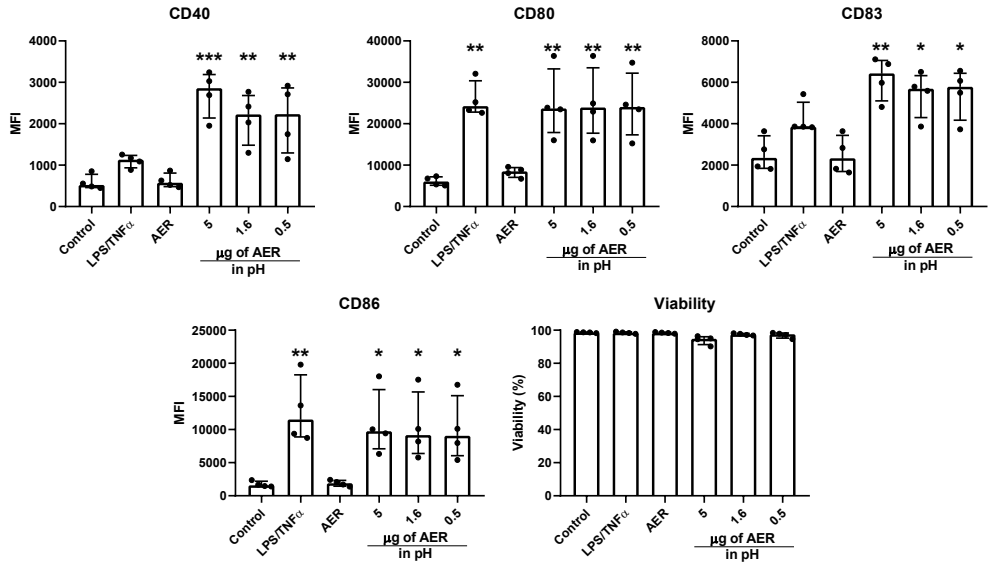

Supplementary Figure S6. Effect of the EPC:DOPE:DOBAQ:DOPC liposomes containing different doses of AER, and CpG and MPLA adjuvants on the expression of cell surface activation markers in primary human monocyte-derived dendritic cells (MDDCs). Median fluorescence intensities (MFI) related to the expression of indicated activation markers: CD40, CD80, CD83, and CD86, n = 4 (cell donors). Cell viability was calculated as a percentage of SYTOX AADvanced -negative cell population in relation to all recorded cells. Formulations were compared to (medium-only) control. The results represent median ± IQR.

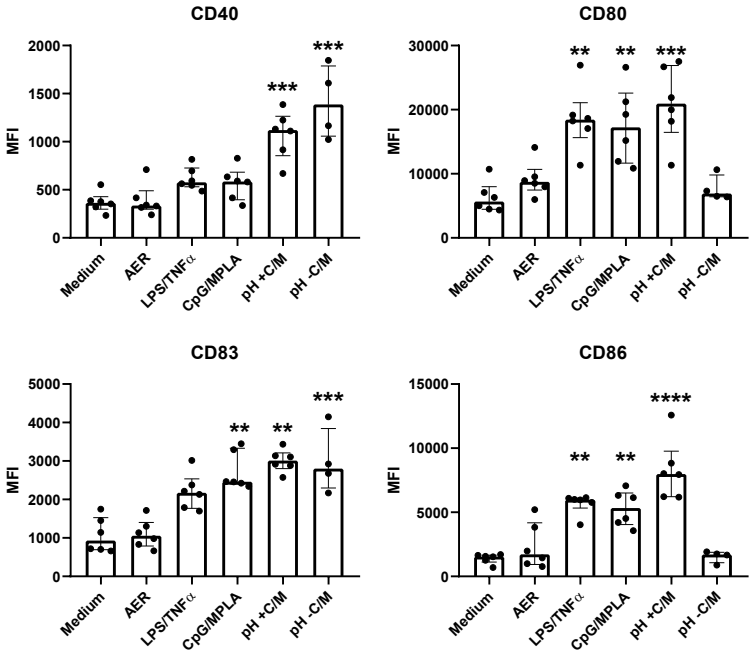

Supplementary Figure S7. Effect of the CpG and MPLA adjuvants on the immunogenicity of EPC:DOPE:DOBAQ:DOPC liposomes containing AER on the expression of cell surface activation markers in primary human monocyte-derived dendritic cells (MDDCs). Median fluorescence intensities (MFI) related to the expression of indicated activation markers: CD40, CD80, CD83, and CD86, n = 6 (cell donors). pH + C/M – liposome containing CpG and MPLA, pH - C/M – liposomes without molecular adjuvants. Formulations were compared to (medium-only) control. The results represent median ± IQR.

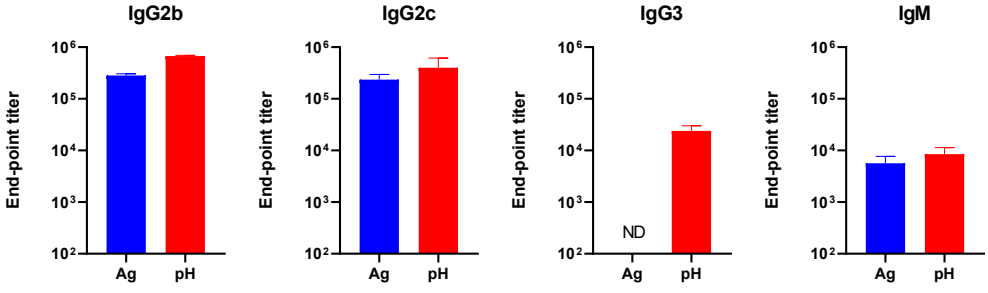

Supplementary Figure S8. Quantification of AER-specific antibodies in sera. The type of antibody measured is indicated above each graph as well as the vaccination group. Values represent end-point titers. Naïve controls were not included because of the undetected (total) AER-specific antibodies (Figure 7). n = 2 (mice).

SUPPLEMENTARY MATERIALS AND METHODS

S1. Generation of Monocyte-derived Dendritic Cells (MDDCs) from Peripheral Blood Mononuclear Cells (PBMCs)

PBMCs were isolated from buffy coats obtained from healthy individuals who provided written informed consent (Sanquin Blood Bank, The Netherlands). The PBMCs were separated using a Ficoll-based density gradient centrifugation method. $CD14^+$ cells were then isolated from the PBMCs using the magnetic cell isolation (MACS) technique with an autoMACS Pro Separator (Miltenyi Biotec BV, the Netherlands).

To generate MDDCs, the isolated $CD14^+$ cells were incubated for six days in the presence of cytokines: 10 ng/ml recombinant human granulocyte-macrophage colony-stimulating factor (GM-CSF; Miltenyi Biotec BV, the Netherlands) and 10 ng/ml recombinant human interleukin-4 (IL-4; Peprotech, USA). The cells were cultured at 37 °C with 5 % CO_2 in complete Roswell Park Memorial Institute (RPMI) 1640 medium, which was supplemented with 10 % fetal bovine serum (FBS), 100 units/ml penicillin, 100 µg/ml streptomycin, and 2mM GlutaMAX (Gibco, Thermo Fisher Scientific, Belgium). MDDCs were harvested by pipetting the medium.

S2. Activation and Viability of MDDCs

To evaluate the cellular toxicity and immunogenicity of AER-containing liposomal formulations in MDDCs flow cytometry analysis was performed. The formulations were added to round-bottom 96-well plates (CELLSTAR, Greiner Bio-One GmbH, Germany) pre-seeded with 30,000 MDDCs per well (250 µg/ml lipids, 0.5-5 µg/ml AER, in 200 µl medium) and incubated for 1 hour at 37 °C with 5 % CO_2. The cells were then washed with complete RPMI medium to remove free liposomes and cultured overnight. The following day, the cells were spun down, and the supernatants were collected and stored at -20 °C to measure cytokine/chemokine production. For flow cytometry staining, the cells were washed with FACS buffer (PBS containing 0.1 % bovine serum albumin; Merck, Germany) and incubated for 5 minutes with 5 % human serum (Sanquin Blood Bank, the Netherlands) in PBS to block non-specific Fc-receptor binding. The cells were then washed, and the cell surface markers on the MDDCs were stained for at least 30 minutes with monoclonal antibodies: CD83-PE (clone HB15e), CD40-APC (clone 5C3), CD80-APC-R700 (clone L307.4)

from BD Biosciences, Belgium, and CD86-BV421 (clone IT2.2) from BioLegend, the Netherlands, in FACS buffer. After staining, the cells were washed and stained with SYTOX AADvanced Dead Cell Stain (Invitrogen, Thermo Fisher Scientific, Belgium) in FACS buffer. Viability was calculated as the percentage of the SYTOX AADvanced-negative cell population relative to all recorded cells. Flow cytometry data acquisition was performed using a BD FACSLyric Flow Cytometer (BD Biosciences, Belgium), and data were analyzed using FlowJo software (version 10.6, FlowJo LLC, BD, USA).

S3. Luminex Assay

Supernatants were analyzed using two Bio-Plex panels (Bio-Rad, Veenendaal, the Netherlands) according to the manufacturer's protocols. A total of 16 analytes were measured. The chemokine panel included CXCL9, CXCL11, CCL8, and CCL22. The cytokine panel consisted of CCL11 (Eotaxin), GM-CSF, IFN-α2, IL-1β, IL-1rα, IL-6, CXCL10, CCL2 (MCP-1), CCL3, CCL4, RANTES, and TNF-α. Samples were acquired on a Bio-Plex 200 system and analyzed using Bio-Plex manager software version 6.1.